Universidad Carlos III de Madrid

Bachelor in aerospace engineering

Academic year: 2017-2018

Bachelor thesis

Design and calibration of turbulent boundary layer wall-shear stress sensor

Author: Pablo Alejandro Pinilla

Supervisor: Alejandro Güemes Jiménez

Leganés, September 22, 2018

Abstract

Turbulent flow measurements are one of the most difficult tasks in fluid mechanics, in particular the characterization of the wall-shear stress. In water media there is little research in the topic. Complete characterization of the shear stress measurements in water environment can really suppose an advance in the design of pipes, pumps even external surfaces of marine vehicles.

The aim of this thesis is to design a device capable of calibrating wall-shear stress sensors in water media. This device will be a plane wave tube (PWT). With the aid of a loudspeaker an oscillatory turbulent boundary layer will be excited at the tube wall and consequently a wall-shear stress will be generated. Measurements will be taken using a hot-film sensor and a microphone.

After the design and manufacture of the PWT. Some recommendations and suggestions about the next steps in the research will be proposed. In the near future static and dynamic calibration could be performed.

Key words: Fluid dynamics, acoustic measurement, fluid flow measurement, calibration, stress measurement, boundary layer, hot-film, manufacturing, plane wave tube.

Acknowledgements

In life, one cannot reach anything alone. Every achievement is directly or indirectly caused by the aid of others. Life a chain of events, in which there is an unstoppable transfer of knowledge, dreams and feelings from one person to another. Even some words, can start this transfer that will propagate through generations from one person to another. The only way to die is to be forgotten. That is why I present this section, as a tribute to the ones that directly or indirectly have contributed, in my case, to the release of this thesis.

First, I want to dedicate this thesis to my family, putting special attention to my parents, who have been there during all my life, specially these four years. They have been watching his little boy grow year to year. They have always believed in me, by celebrating my achievements and consoling me in my defeats. I want you to be proud of all your effort and time invested.

Dedicated to my girlfriend Cristina, you have been with me during the whole the bachelor, making these years the best of my life. You are one of those reasons which make fight worth for. There are not enough words to quantify how you have contributed to this and to my life.

Dedicated to my friends from Zamora: Pablo, Diego, Miguel and Alberto. Since we were little children we were dreaming to become adults. Hope those little kids could watch us who we have become now.

Dedicated to all the people I got to know here in the UC3M, especially Pablo and Fernando. Not so long ago we were rookies discovering Madrid and now a crossroad seems to appear in the horizon.

Thanks to all the teachers that I had in my home school. They set the basis of the curious man that I am now. I really feel grateful of having had them as teachers. Perhaps, things could have not been the way they have happened if I had not studied in that school.

Thanks to all the academic staff in the UC3M, specially the aerospace engineering department. You have always been open to solve any doubt with a smile in your faces.

Thanks to Prof. Andrea Ianiro and Prof. Stefano Discetti that offer me the chance to do this thesis when I was outside of Spain and for all the wisdom, knowledge and support given.

I want to thank Carlos Cobos for his time, advice and dedication during the post-machining process of the project. His practical knowledge in the workshop was very useful for the realization of the thesis setting a basis for future ones. He was always free to gently explain tool working and processes with a big smile and some jokes.

Particularly, I want to thank my tutor, Alejandro Güemes. He has been instructing and correcting me week by week. He has been very patient and encouraging with me. We have been working, suffering and celebrating together during all these months. He is the one that specially knows how hard I have worked. Without him it would have been virtually impossible for me presenting this thesis.

Lastly, thanks to all the future readers of this thesis. You are the ones those who will spread the knowledge to the future.

Contents

List of Figures

List of Tables

List of Symbols

L_c Characteristic length

Re Reynolds number

Stk Stokes number

U_c Characteristic velocity

α Foam absorption coefficient

δ^* Displacement thickness

ϵ Energy transfer rate

η Kolmogorov length scale

μ Dynamic viscosity

ν Kinematic viscosity

ω Angular frequency

ρ Density

τ_w Wall-shear stress

τ_η Kolmogorov velocity scale

θ Momentum thickness

a_T Overheat ratio

d PWT side length

k Wave number

l_t PWT length

p Pressure

u Horizontal velocity

u_τ Wall velocity

u_e Freestream velocity

u_η Kolmogorov velocity scale

v Vertical velocity

w Transverse velocity

1 Introduction

Richard Feynman said once [1]: *"There is a physical problem that is common to many fields, that is very old, and that has not been solved. Nobody in Physics has really been able to analyze it mathematically satisfactorily in spite of its importance to the sister sciences. It is the analysis of circulating or turbulent fluids."*

Turbulent flows are present everywhere, from the shy smoke of a cigar to the huge clouds of the sky, from the violent geysers in the volcanic regions to a simple jet stream in the washing basin of a house. Even empirically, one can deduce the chaotic behaviour of this kind of flows compared with other branches of the mechanics. For instance, in classical mechanics given the initial conditions and the forces over a body, the whole trajectory of the motion can be determined with very small errors. This means that classical mechanics is a deterministic science. On the other side, turbulent fluid mechanics can be considered a non deterministic branch of mechanics; this means that systems governed by turbulence present extremely high sensitivity to changes in initial conditions so prediction is uncertain. When the meteorologist Edward Lorentz was studying the atmosphere convection [2] -a turbulent phenomenon- discovered that even that the motion was extremely chaotic, fluid particles tend to group into fixed structures, what he called strange attractor. This established the basis of chaos theory what became a powerful tool in turbulence research and modelling. Some scientists even believe a possible deterministic approach for turbulent flows [3]. Until that hypothesis is verified, statistics is used as a tool to analyse turbulence.

Through the recent history, in turbulent fluid mechanics, there has been a great interest in studying wall-bounded flows, that is, flows that are surrounded by solid boundaries. In this classification the well-known three canonical problems of the turbulent flow are included. These are the zero pressure gradient turbulent boundary layer (ZPG TBL), the turbulent channel flow (TC) and turbulent pipe flow (TP). Since these problems were proposed, there has been a lot of research on the topic [4] because of their inertly evident direct application in industry and engineering. By studying how the shear stress in pipes or channels develops, it is possible to generate accurate roughness distributions in the pipes in order to minimize losses.

For the research, there exist some numerical methods that allow scientists and engineers to simulate models of turbulent flows and compare them to reality. Direct Numerical Simulation (DNS) techniques implement directly the Navier-Stokes equations for all the scales of the flow. However, DNS requires extremely large computational times and memory storage so they can only be used to study simple flows at moderate Reynolds numbers. Because of this, experiments have become the only valuable option that scientists have to simulate high Reynolds number turbulent flows. In any case, the inherent complexity of these energetic flows makes experimental simulations a tough task. As the Reynolds number is increased, the range of eddies scales is increased, and thus with the typical measurement techniques, perturbation in the results is unavoidable. These errors arise (even without taking into account physical interference with the sensors) because small eddies are integrated by sensors as an average and not individually because the length scale of typical sensors is much larger than the eddy itself. Some experiments using high viscosity

flows in order to increase the dimensions of the eddy length scale were tried. Nevertheless, because of viscosity, only experiments at low Reynolds numbers could be performed being extrapolation to the turbulent regime difficult.

During the major part of the last century only hot-film and hot-wire anemometers were used to characterize turbulent flows. This simple devices make use of resistors to adjust to changes in temperature in the film/wire and thus measure fluctuations in the flow. Currently, particle image visualization (PIV) is being used to accurate describe velocity distributions of fluid flows in wind tunnels. This technique uses very powerful lasers in order to illuminate seeder particles that are placed in the flow to compute its velocity field in a non intrusive way. Nevertheless, although the accuracy of this method is high, the use of PIV techniques requires a large investment of money. At the end of last century, the development of Micro Electro-Mechanical Systems (MEMS) led to a revolution in fluid mechanic measurements. MEMS sensors allow scientists to measure fluid properties in the Kolmogorov scale and therefore without disturbing the results. Most of them could be mass-produced so the cost per unit sensor could be sharply reduced. This technology is quite new and is still being used to characterize turbulent flows. The fact that there is little research yet on fluids other than air, makes it reasonable to use MEMS sensors to investigate in the water media in the recent future. However, as even the less complex MEMS are currently under investigation in air, it is convenient to make a more comprehensive and deeper study of the classic hot-wire and hot-film problem in water media -a more challenging media than air- in order to make the further step of MEMS to water media. The characterization of the shear stress distribution in water media is a key element for instance in naval industry in which there is a constant exposure of surfaces to unsteady water flow. Research on the topic in the future may lead to optimization of naval structures such as submarines, ships or offshore wind turbines.

In this thesis a method for the calibration of a conventional turbulent boundary layer shear stress hot-film sensor will be discussed by means of a water plane wave tube and the Stokes layer excitation. Particularly in this thesis, the design and manufacturing process of the experiment components will be extensively discussed. In addition, some suggestions and recommendations for future researchers will be provided. The future experiment will consist on generating a known fluctuating pressure field that due to the non slip condition at the tube wall will induce a frequency dependant boundary layer that will produce a known shear stress distribution at the tube wall. This known shear stress will be related to the voltage measured by the sensor in order to perform the calibration.

In the following analysis a local coordinate system centered in the axis of the tube and located in one side of the tube will be used. In this coordinate system the x axis coincides with the tube axis whereas y and z are aligned with the height and the width of the cross section. Moreover, u, v and w will stand for the velocities along the x, y and z directions respectively.

Chapter 2 will introduce some background and formulation to further understand the problem proposed. Chapter 3 is the gross part of the thesis, it extensively explains and develops the design and manufacturing process of the PWT and its related components. Chapters 4 and 5 derives some conclusions, recommendations

and ideas for future researchers. Additionally Chapter 6 includes a time line of the project planning. Appendix A: Budget analyses carefully all the related costs of the project. Appendix B: Dimensions presents all the technical drawings of the parts involved in the final version of the project. Appendix C: Datasheets includes technical information of the most important electronic devices of the project. Additionally, Appendix D: Test protocol provides some helpful insight for the future experiments. Finally, the socio-economical background and legal framework are presented later in this section.

1.1 Socio-economical background

To move water from one place to another is redundant since ancient times. At the beginning of history wooden pipes were used to distribute water to the crops, later on, Romans built the famous aqueducts to displace the fluid from large reservoirs outside of the cities. But one of the largest innovators in terms of water canalization were the Arabians, prove of that is their amazing masterpiece in the Alhambra (Granada). Hundreds of canals distributed along the monument feed fountains and gardens. Soon sewing systems become common in cities and finally water came to the houses magically by opening simply a valve.

Figure 1: Alhambra channel. Courtesy: Patronato de la Alhambra y el Generalife

Figure 2: Segovia aqueduct. Courtesy: National Geographic

As it is visible by looking at the previous examples in Figures 1 or 2, water damages the container along which it flows making part repairing and replacing a repetitive and expensive task. Every time a bifurcation or a change in cross sectional area in a pipe appear, damage is enhanced even more. Nowadays, technology imposes harder requirements to fulfill in terms of costs and forces constraints. To be able to minimize the friction losses -and hence pressure losses- in a pipe could

mean cost savings. In addition, to reduce the wall-shear stress loading in every cycle could mean less part replacing due to fatigue failures. This project could be used by pipe and canal manufacturers to determine the shear stresses and at some extent friction losses. Companies could calibrate their own wall-shear stress sensors in a very cheap way saving hundreds of euros.

Similarly, using the same approach, pump and water turbine manufacturers can use this method to calibrate their wall-shear stress sensors. In pumps and turbines the determination of the wall-shear stress is even more critical because of the large speeds and the rotational effects. Interference effects between the different blades, and cavitation provoke a complex distribution of velocities and pressures what makes wall-shear determination a complex task what is transcribed in high cost. Whatever cost reduction would lead to money saving that could be used to improve measurement quality in that complex environment.

Last but not least, this project could also be used in the naval industry. As a conceptual approach, the shear stress sensors could detect shear stress levels in the surface of critical parts of the boat hull or more critically of the external surface of a submarine. Shear stress is directly related with the drag distribution of the body, so minimizing it is beneficial in both the performance and structural point of view. So to measure and to control its magnitude in any moment during a mission could optimize the performance and the life of the vehicle. By placing shear stress sensors in key points of the vehicle a detailed model of the drag distribution could be obtained. A real time display of the stress distribution could be shown in the cabin. When the pilot notices negative levels of shear stresses, he could deflect different control surfaces or activate boundary layer suction mechanisms to alleviate at some extent the drag distribution around the body. But those sensors should have been checked previously so they work properly. That is where this thesis has direct application in a similar way as previously discussed.

To sum up, a low cost method to calibrate shear stress sensors in water media would be proposed. This thesis has direct consequences in whichever engineering application related with water distribution and motion. The concept could be used by different engineering companies to test shear stress sensors in a cheap way without the need of very complex and expensive hydrophones. The fact that most of the components can be 3-D printed can really decrease the maintenance cost of the apparatus. When some component becomes damaged it could be replaced by simply printing it again. For the cost of the main structure as it is made of PVC instead of metal the manufacturing cost can decrease considerably.

1.2 Legal framework

Basically this experiment has been developed according to 2 standards. These are ISO 10534-2:1998(E) and ASTM E1050-12. For the case of amortization, the Spanish government imposes some legislation included in BOE-A-2014-12328 [5]. The latter one is not included here but can be easily accessed in the BOE website. The main restrictions imposed by these documents are presented below.

1.2.1 ISO 10534-2:1998(E)

- ≪For rectangular tubes the corners shall be made rigid enough to prevent distortion of the side wall plates. It is recommended that the side wall thickness be about 10 % of the cross dimension of the tube.≫

- ≪The loudspeaker generally will produce non-plane modes besides the plane wave. They will die out within a distance of about three tube diameters or three times the maximum lateral dimensions of rectangular tubes for frequencies below the lower cut-off frequency of the first higher mode. Thus it is recommended that microphones shall be located no closer to the source than suggested above, but in any case no closer than one diameter or one maximum lateral dimension, as appropriate.≫

- ≪The surface of the loudspeaker membrane shall cover at least two-thirds of the cross-sectional area of the impedance tube.≫

1.2.2 ASTM E1050-12

- ≪In order to maintain plane wave propagation, the upper frequency limit is defined as follows:

$$f_u < \frac{K\ c}{d} \tag{1}$$

  where:
  f_u = upper frequency limit, hertz,
  c = speed of sound in the tube, m/s,
  For rectangular tubes, d is defined as the largest section dimension the tube and K is defined as 0.500.≫

- ≪The sound sources should have a uniform power response over the frequency range of interest. It may either be coaxial with the main tube or joined to the main tube by means of a transition having a straight, tapered, or exponential section.≫

- ≪It is desirable to mount both microphone diaphragms flush with the interior surface of the tube using port openings through the side of the tube.≫

2 State of art

2.1 Boundary layer

The boundary layer is a transition zone between the freestream flow and the zero velocity at the wall due to the non slip condition. In this zone viscous effects are important. In fluid mechanics the main boundary layers are the velocity and temperature boundary layers. The Navier-Stokes equations for incompressible flows have 4 unknowns: the three velocity components u, v, w and the pressure p. Using scale analysis, Prandtl proved that pressure is isobaric in the wall-normal direction [6]. With this approximation the two-dimensional Navier-Stokes equations reduce as follows:

$$\frac{\partial u}{\partial x} + \frac{\partial v}{\partial y} = 0 \tag{2}$$

$$\rho\frac{\partial u}{\partial t} + \rho u\frac{\partial u}{\partial x} + \rho v\frac{\partial u}{\partial y} = -\frac{\partial p_e}{\partial x} + \mu\frac{\partial^2 u}{\partial y^2} \tag{3}$$

Where ρ and μ are the density and dynamic viscosity of the fluid. The main parameters used to describe the velocity boundary layer are the displacement thickness δ^* and the momentum thickness θ. δ^* is the distance that the wall have to be theoretically displaced in order to have the same mass flow as the lost one due to the presence of the boundary layer. Moreover, δ^* can be interpreted as the upward deflection of the streamline external to the boundary layer due to the partial blockage of the freestream flow provoked by the retarded flow inside the boundary layer. Similarly, θ accounts for the distance that the wall should be moved in order to have the same momentum as the lost due to the presence of the boundary layer. The equations that describe δ^* and θ are:

$$\delta^* = \int_0^\infty \left(1 - \frac{u}{u_e}\right) dy \tag{4}$$

$$\theta = \int_0^\infty \frac{u}{u_e}\left(1 - \frac{u}{u_e}\right) dy \tag{5}$$

In which u_e represents the freestream velocity. The wall-shear stress τ_w is directly proportional to the derivative of the velocity parallel to the wall.

$$\tau_w = \mu \left.\frac{\partial u}{\partial y}\right|_{y=0} \tag{6}$$

The friction velocity u_τ is determined by:

$$u_\tau = \sqrt{\frac{\tau_w}{\rho}} \tag{7}$$

According to the energy contained, boundary layers can be classified into laminar and turbulent boundary layers depending of the Reynolds number (Re). The Re is a non dimensional number that relates inertial to viscous forces.

$$Re = \frac{\rho\ U_c\ L_c}{\mu} \tag{8}$$

Where U_c and L_c are the characteristic velocity and length respectively. For low Reynolds numbers, when the flow is slightly perturbed, properties such as velocity or pressure are steady -at constant distances from the wall- in the direction perpendicular to the solid wall. A laminar boundary layer is formed.

However if the Reynolds number is increased, non linear contributions in the velocity induce an unsteady behaviour, a turbulent boundary layer appears. This layer has more kinetic energy than his laminar counterpart and therefore is more difficult to be detached from the wall.

2.2 Scales

The complexity of the turbulent flow makes convenient to divide the boundary layer in several regions [7] [8]:

- **Outer boundary layer**: in which the flow behaves as a free shear flow. A new coordinate system can be posed using as reference length the boundary layer thickness δ:

$$\bar{y} = \frac{y}{\delta} \tag{9}$$

- **Inner boundary layer (Constant stress layer)**: in which the shear stress can be considered constant. In this zone the considered coordinates are:

$$y^+ = \frac{y\ u_\tau}{\nu} \tag{10}$$

  This layer is divided into:

  - Linear sublayer: $0 < y^+ < 3$
  - Buffer sublayer: $3 < y^+ < 30$
  - Meso sublayer: $30 < y^+ < 300$

The schematics of the different layers are shown in Figure 3.

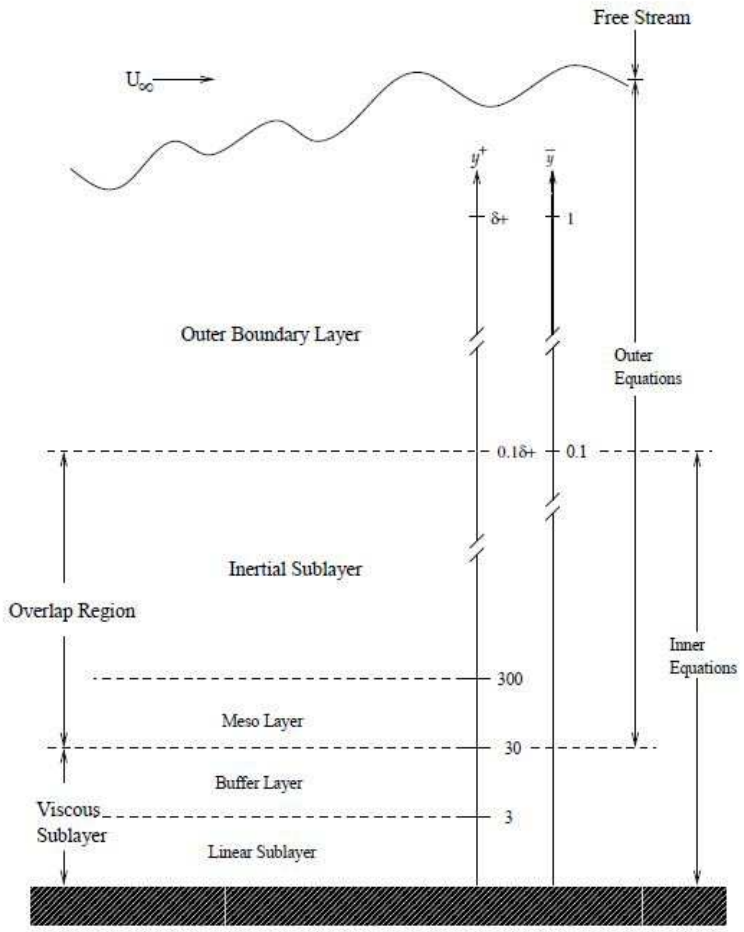

Figure 3: Schematics of the different layers and sublayers in a turbulent boundary layer. Courtesy: William K. George.

To fully characterize the nature of the eddies in the turbulent regime, measurements in the order of micrometers have to be performed. For this reason, usually microscales are used for non dimensional analysis, one of these scales is known as Kolgomorov scale.

Large eddies present high Reynolds number due to the high contribution of convective terms. However, large eddies are very unstable and break naturally into smaller eddies, and so successively to the very smallest eddies in which viscosity is very important and the Reynolds can be considered of order unity reaching a stable configuration. Kolmogorov [9] discovered that this process was fully determined by the kinematic viscosity ν and the energy transfer rate ϵ. Thus he defined the length η, velocity u_η and time τ_η scales named after him:

$$\eta = \left(\frac{\nu^3}{\epsilon}\right)^{\frac{1}{4}} \tag{11}$$

$$u_\eta = (\epsilon\nu)^{\frac{1}{4}} \tag{12}$$

$$\tau_\eta = \left(\frac{\nu}{\epsilon}\right)^{\frac{1}{2}} \tag{13}$$

2.3 Stokes layer excitation

The Stokes layer is a type of boundary layer in which the upstream flow presents an oscillatory character. By inducing an oscillation in the upstream velocity a frequency dependant boundary layer is generated. Chandrasekaran [10] found some analytical solutions for the Stokes problem in a rectangular tube of cross section $2a\ x\ 2b$. The geometry of the problem is shown in Figure 4:

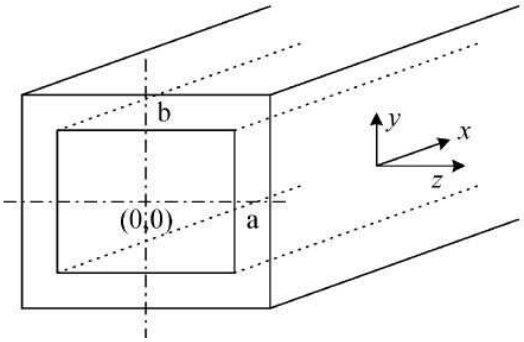

Figure 4: Geometry of the problem. Courtesy: Chandrasekaran (2005)

The Navier-Stokes momentum equation to be solved is:

$$\frac{\partial u}{\partial t} = -\frac{1}{\rho}\frac{\partial p}{\partial x} + \nu\nabla^2 u \tag{14}$$

Assuming a known pressure distribution:

$$p = p^{'} Re\left[e^{j(\omega t - kx - \pi/2)}\right] \tag{15}$$

Where $p^{'}$, k and ω are the amplitude of the perturbation velocity, the wave number, and the angular frequency respectively. The velocity distribution is of the form :

$$u = u^{'} Re\left[e^{j(\omega t - kx - \pi/2)}\right] \tag{16}$$

The perturbation velocity $u^{'}$ has to fulfill the non slip condition at the tube wall:

$$u^{'}(z = \pm a) = 0 \qquad u^{'}(y = \pm b) = 0 \tag{17}$$

Introducing the Stokes number Stk as the non dimensional number that relates the frequency of the periodic perturbations to the length scale:

$$Stk = \sqrt{\frac{\omega\ b^2}{\nu}} \tag{18}$$

According to Chandrasekaran the relevant solution for $Stk > 2$ is one dimensional, that is $a >> b$. Introducing the speed of sound c, $u^{'}$ at the center of the tube for $a >> b$ is:

$$u^{'} = \frac{p^{'}}{\rho c} e^{j(\omega t - kx - \pi/2)} \left\{ 1 - \frac{\cosh\left((y/b) Stk\sqrt{j}\right)}{\cosh\left(Stk\sqrt{j}\right)} \right\} \tag{19}$$

Which leads to a fluctuating wall-shear stress of the form:

$$\tau_w = \frac{p^{'}\sqrt{j\omega\nu}}{c} e^{j(\omega t - kx - \pi/2)} \tanh\left(Stk\sqrt{j}\right) \tag{20}$$

2.4 Plane wave tubes

Plane Wave Tubes (PWT) also called impedance tubes or Kundt tubes are commonly used in acoustics. They are used to completely characterize the transmissive and absorptive properties of materials for their application as sound attenuators. By placing the test material on one side of the tube, a wave source in the other side and several microphones, some important coefficients that are related with reflection and absorption properties of the test material can be measured [11]. Moreover, this devices can be used for fluid mechanic measurements. Different researchers have used PWT for the calibration of wall-shear stress sensors. Sheplak [12] solved the induced shear stress distribution in a cylindrical tube and he dynamically calibrated a floating type shear stress sensor. Gad-el-Hak [13] extensively discussed different types of MEMS shear stress sensors and stablished correlations for the wall-shear using PWT. Chandrasekaran [10] performed a similar analysis but using a square sectional PWT.

However, when switched to water media, research on the topic is quite scarce, due to the inertly more complex environment to perform measurements. Anyway, historically, there was a need for the characterization of water properties. For instance, in the Second World War there was a need for the Germans to develop absorbent materials for their submarines not to be detected by enemies radars. Several studies on sound propagation on water media have been performed in quite sophisticated and expensive plane wave tubes using complex piston systems and transducers [14] [15] [16].

The two principal standards and design keypoints are englobed in the ISO [17] and ASTM [18] documents. The PWT dimensions are completely determined by the operative frequency range. The lower threshold limits the length of the tube l_t whereas the upper one established the side d of the cross section.

$$f_{low} = \frac{c}{4\ l_t} \tag{21}$$

$$f_{high} = 0.5\ \frac{c}{d} \tag{22}$$

In the experiment, the loudspeaker will generate waves in a given range of frequencies. When the frequency generated matches the natural frequency of a specific normal mode, resonance in that mode will happen. To obtain a clear plane wave distribution, non planar wave propagation modes should be avoided. It is required to get rid of those normal modes in the range of operative frequencies of

the tube. These residual vibrational modes have little effect in air media, but for a more dense media like water their effect could be critical. Corbett [19] derived detailed equations for high order modes in water PWT. According to the standards [17] [18], the wall thickness for a plane wave tube should be at least 10 % of the side of the square section to obtain enough stiffness to damp possible vibrational modes. This is even more critical for water plane wave tubes, in which is needed a material with higher stiffness. From previous experimentation it is recurrent to use stainless steel. To make sure that only plane waves are measured, the standards [17] [18] recommend for the microphones and the sensors to be located at least at 3 diameters from the source of the propagating waves.

As the tube is finite, when the generated wave reaches the end of the tube it is reflected backwards. This new wave will encounter the main propagating wave forming a standing wave what may affect the local flow properties, perturbing the results. Therefore, in the termination of the tube, a foam wedge is placed to mitigate the reflections by absorbing the acoustic energy. This kind of acoustic foams are open celled enabling the sound wave to come through and at the same time to be reflected in the porous cavities. These absorbers are only effective at a given range of frequencies [20], so better results would be expected in the specified frequency range. The main parameter that defines this kind of absorber materials is the absorption coefficient α that depends on the specific frequency, the material, the surface distribution of the pores and the overall geometry of the absorber.

3 Experimental set-up

The next subsections describe separately the components of the experiment. It is remarkable that the design of the plane wave tube was a dynamic process due to adaptability and optimization reasons. This design was a continuous unified process in which whenever a modification in one component was performed, other subsequent and necessary modification in other component was required while at the same time, cost was tried to be reduced as much as possible. This made the set-up a very complex part of the project. Many modifications are omitted from the thesis because of simplicity, only the main ones will appear in the next sections.

3.1 Sensing elements

The two devices used to measure the perturbations are the microphone and the hot-film sensor. The hot-film is the device to be calibrated whereas the microphone is the apparatus needed to perform the calibration process.

Hot-film sensors are based on the variation of the temperature across the sensor. They are composed of a metallic layer into a substrate. The film will be maintained at a higher temperature than the one of the fluid around it what will produce a heat flow between the film and its surroundings: convection heat transfer from the film to the water and conduction heat transfer from the film to the substrate. These sensors can operate in two modes: Constant Temperature Anemometry (CTA) and Constant Current Anemometry (CCA). For convenience, the sensor will operate in CTA mode. Thanks to a Wheatstone bridge, a variable current is transmitted to increase the temperature to compensate for the heat loss from the hot-film to the fluid and to the substrate. Changes in current intensity imply changes in voltage what can be related to the velocity and shear stress. A critical parameter involved is the overheat ratio a_T. It involves the relationship between the temperature difference between the film and its surroundings to the temperature of the surroundings. It is defined as:

$$a_T = \frac{T_f - T_{sur}}{T_{sur}} \tag{23}$$

For the experiments a Senflex© 93111 hot-film sensor will be used. It is a surface array of sensors formed by a Nickel layer elements of 0.001"x 0.057" and 0.2 μm thickness into a polyimide substrate connected using Copper leads. The schematics of the sensor array are shown in Figure 5. To perform the experiments the array was divided into separated hot-film sensors to be calibrated.

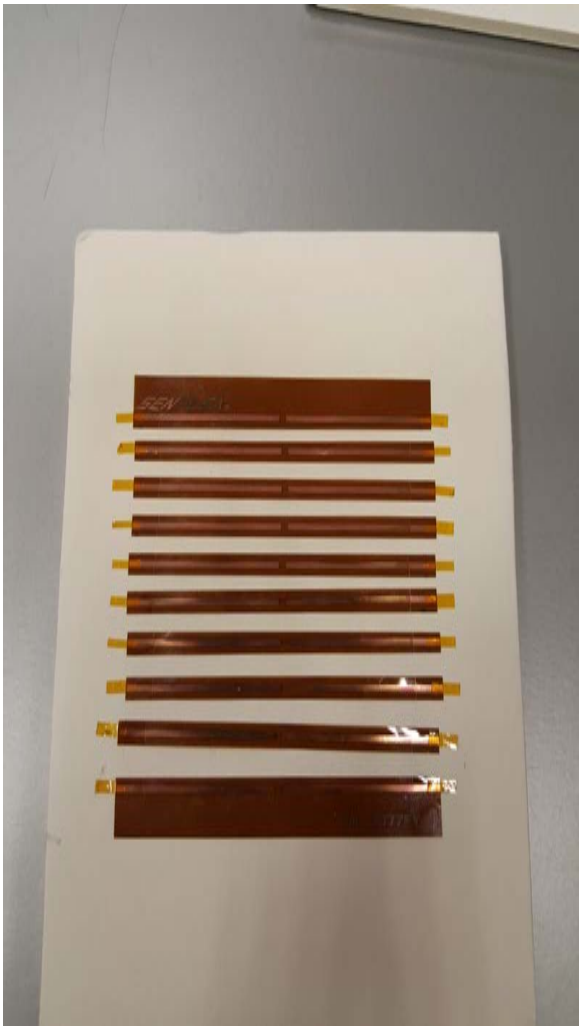

Figure 5: Schematics of the Senflex© 93111 sensor

There were a lot of choices for the decision of the waterproof microphone. These involved from the cheap options like a condenser microphone sealed from water with a rubber membrane to the expensive hydrophones that are used in sea life control capable of the detection of sounds at extremely high frequencies in very extreme environments.

Three are the main performance properties that were checked in the microphone:

- **Sensitivity**: describes how the microphone reacts in terms of voltage when a pressure change acts in the microphone. It is measured in dB/V.
- **Directionality**: takes into how the microphone performance changes with direction of the incoming source. It is described by the polar diagram. For the experiment an onmidirectional microphone is preferred.
- **Frequency response**: describes the behaviour of the microphone for a given frequency range, for the sake of the experiment it is looked for a flat frequency response as all the frequencies are important.

Additionally, because of the aim of extremely high accuracy, it is required for the microphone to be as small as possible in order to perform the measurement of the signal as close as possible to the cross section in which the hot-film sensor measures. This is because the microphone measures performing an average in the pressure distribution in the membrane. Thus, the larger the microphone, the less convenient for the experiment. The more the microphone represents a measuring point, the better, so very small planar microphones were required.

On one hand, condenser microphones involve a fix plate and a movable plate that is sensitive to changes in pressure. Changes in pressure, involve changes in the distance between the plates.This changes condenser capacity with the subsequent change in voltage. Condenser waterproof microphones are presented in different geometries and sizes but they are required to be driven with an external circuit. Additionally, they are cheap and affordable.

On the other hand, hydrophones are usually presented as capsular probes in which the sound comes in a onmidirectional way. There exist planar hydrophones but their size exceeded the one required for the experiment. The main advantage of this kind of devices is their accuracy and warranty of success, whereas the main drawback is the extremely high cost that involves the probe and the microphone amplifier.

Given the constraints of the experiment it was decided to use a condenser waterproof microphone. The model used is POW-1644L-LWC50-B-R for which the data sheet is included in Appendix C: Datasheets. The microphone model is shown in Figure 6. As stated previously these condenser microphones require an external driving circuit in order to obtain enough power and amplification for the the signals to be measured and analyzed.

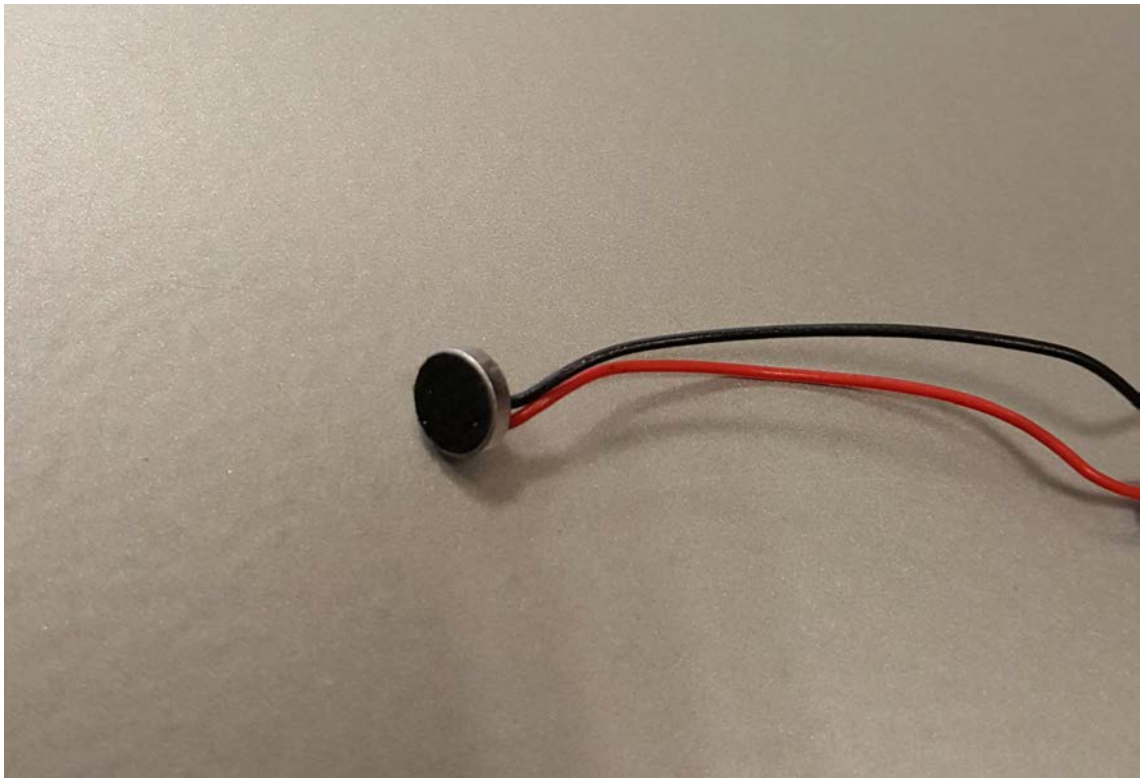

Figure 6: POW-1644L-LWC50-B-R microphone

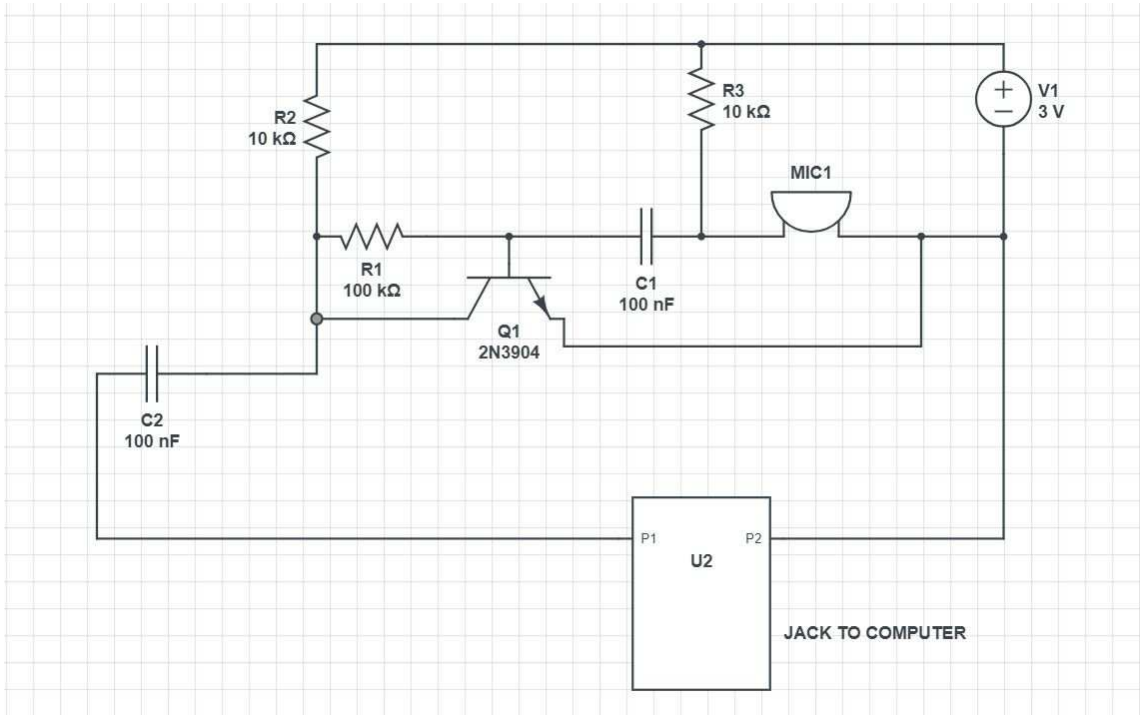

Figure 7: Driving circuit

Figure 8: Sound card

Figure 9: Tin welder and tin for welding

The driving circuit is sketched in Figure 7. It consists on a supply voltage of 3 V, 3 resistors to restrict the current flow through the microphone, 2 capacitors to add some AC coupling and improve the quality of the signal an finally a 2N3904 transistor that works in this case as an amplifier. It was needed a breadboard to female jack connector, a male jack to male jack connector and a external sound card to connect the circuit to the computer like the one shown in Figure 8. To attach some lags to the different components tin welding was used. The tin welding probe and the tin supply are shown in Figure 9. To increase the quality of the weld some rust-removing fluid was used. It is highlighted that in order to test the circuit another condenser microphone with a similar power requirements was used to avoid possible damages on the test microphone. Schematics of both the test and the actual circuits are shown in Figures 10 and 11. To test the microphones a frequency sweep signal was recorded using "Audacity" software and processed in "Matlab". An example of the microphone test is shown in Figure 12.

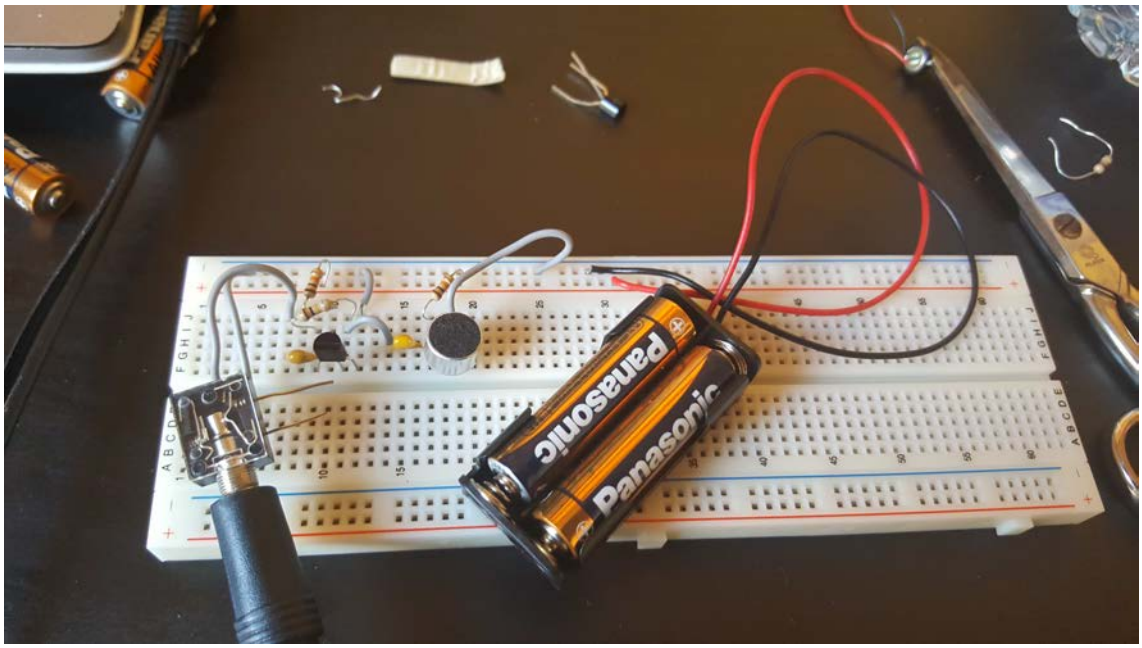

Figure 10: Test circuit with auxiliar microphone

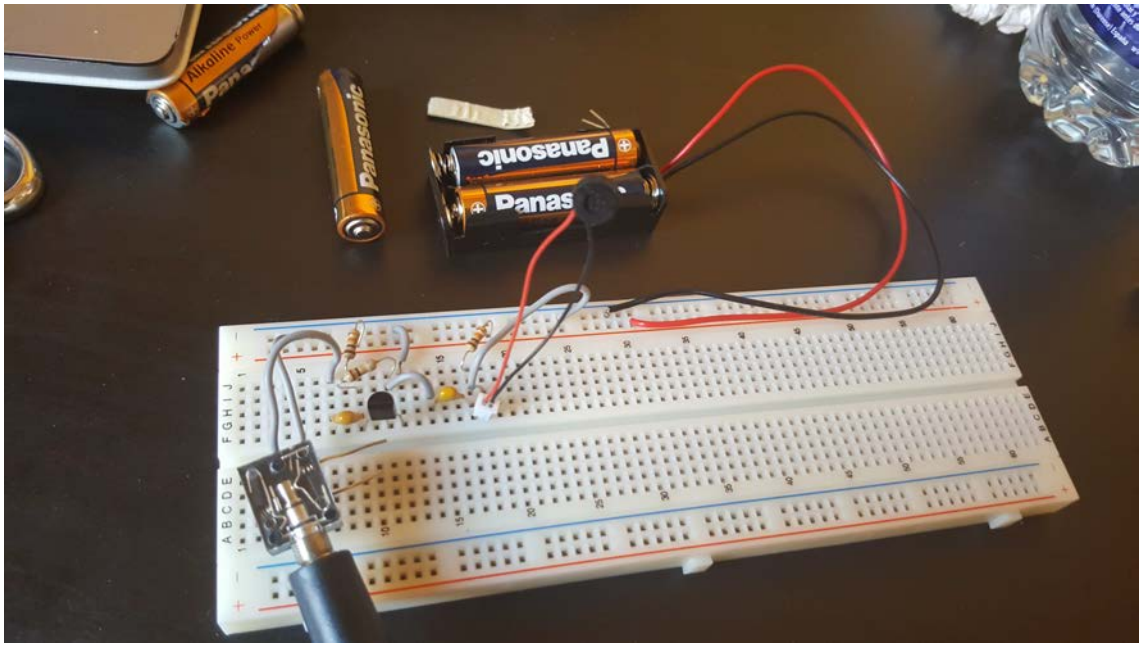

Figure 11: Test circuit with actual microphone

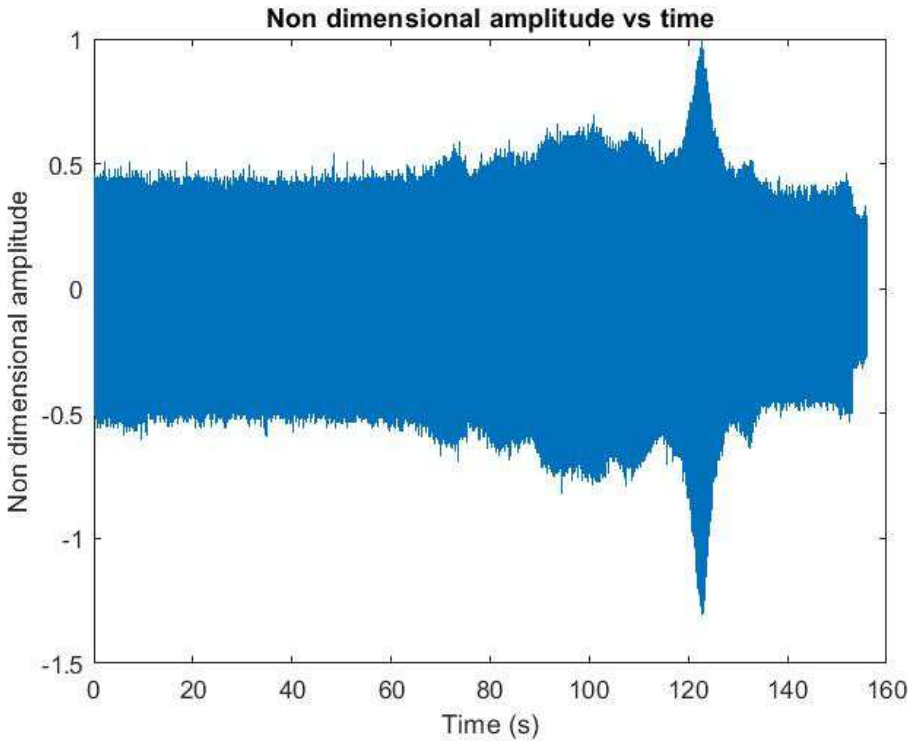

Figure 12: Audio recording test with the actual microphone

Once the microphone was tested in the air media it was needed to prove its waterproof properties, therefore a new test was to be carried out. The set up of the experiment is shown in Figure 13. It consists on the same circuit as the air test, a container filled with stagnant water, an old mobile phone, and a protective cover for

the old mobile phone. The microphone membrane was submerged some millimeters parallel to the floor. The results of the test were promising, for the same power conditions of the air experiment the microphone was able to sense larger amplitudes although some perturbations were obtained. This is obviously explained because of the variation in density and sound speed with respect to air media. Audio recording results of the test are shown in Figure 14.

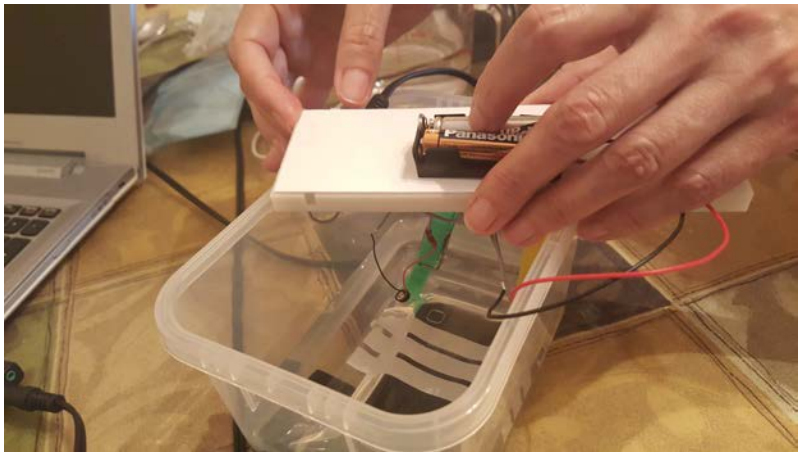

Figure 13: Water microphone test set-up

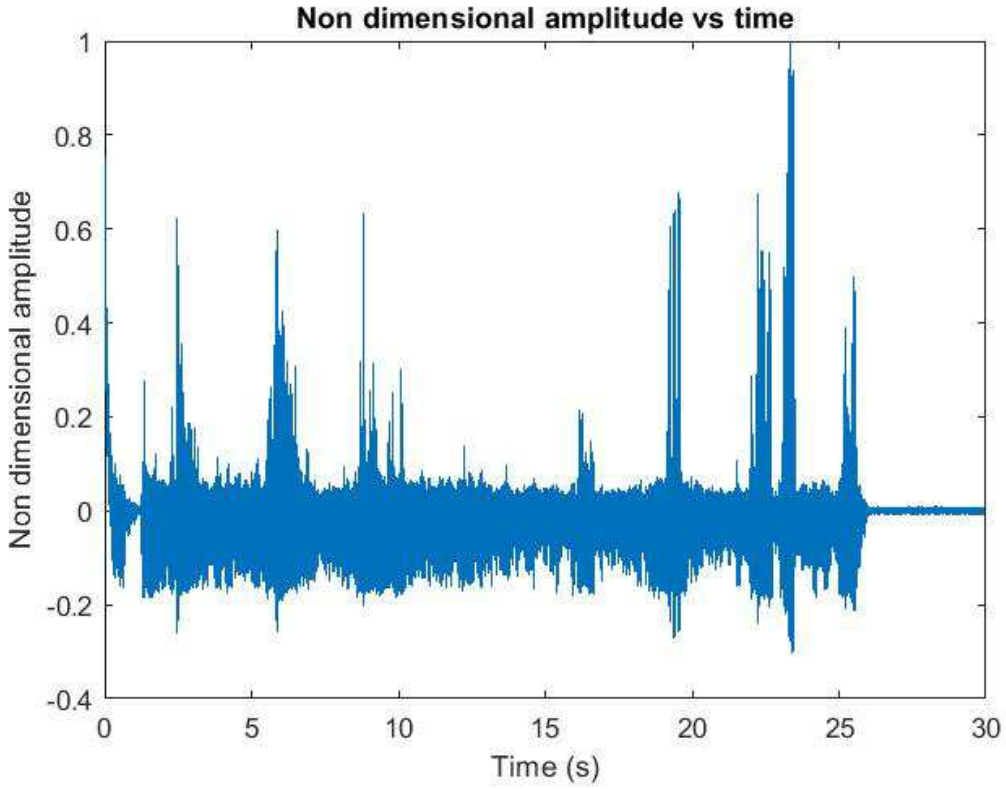

Figure 14: Water test recording results

3.2 Source of the excitation

The decision of the source of the excitations was neither an easy task. On one hand different experienced researchers [21] [22] recommended using a piston mechanism to produce the boundary layer excitations in the water environment. Different models of linear actuators were investigated, but in addition to the high costs, some factors like lubrication, mechanical losses and -above all- frequency range limitations were critical to discard this option. Therefore the choice of using a loudspeaker appeared as prime option. The main performance parameters taken into account were again the sensitivity and frequency response being this one less critical. At first, it was proposed to use a loudspeaker of approximately the same cross section as the one of the tube. However, the scarce of loudspeaker models that fulfilled the frequency requirements made it reasonable to use a larger one. Finally the chosen model was PYLE© PLMRW8 usually used in car applications and it is shown in Figure 15. The datasheet of the is included in Appendix C: Datasheets.

Figure 15: PYLE© PLMRW8 loudspeaker

For the proper operation and functioning of the loudspeaker a signal generator was needed. This device produces predefined signal outputs depending of the parameters set. The chosen model is a RIGOL DG4062 signal generator shown in Figure 16. To check proper working of the loudspeaker, a preliminary frequency sweep was performed in a conservative frequency range. The signal generator produced in a period of 10 seconds a logarithmic sweep from 200 Hz To 20 KHz. To easily notice when the test signal is finished the start and end frequencies were played for an additional 3 seconds each. For safety measures the amplitude of the signal was set to 3 V not to surpass the threshold of pain of hearing as it decreases with increasing frequency [23]. To connect the loudspeaker with the signal generator a BNC wire was needed to be manufactured in the university workshop. The set-up of this preliminary test is shown in Figure 17. When it was performed the loudspeaker was shown to work perfectly. As a summary, Table 1 shows the principal electronic devices in the project

Figure 16: RIGOL DG4062

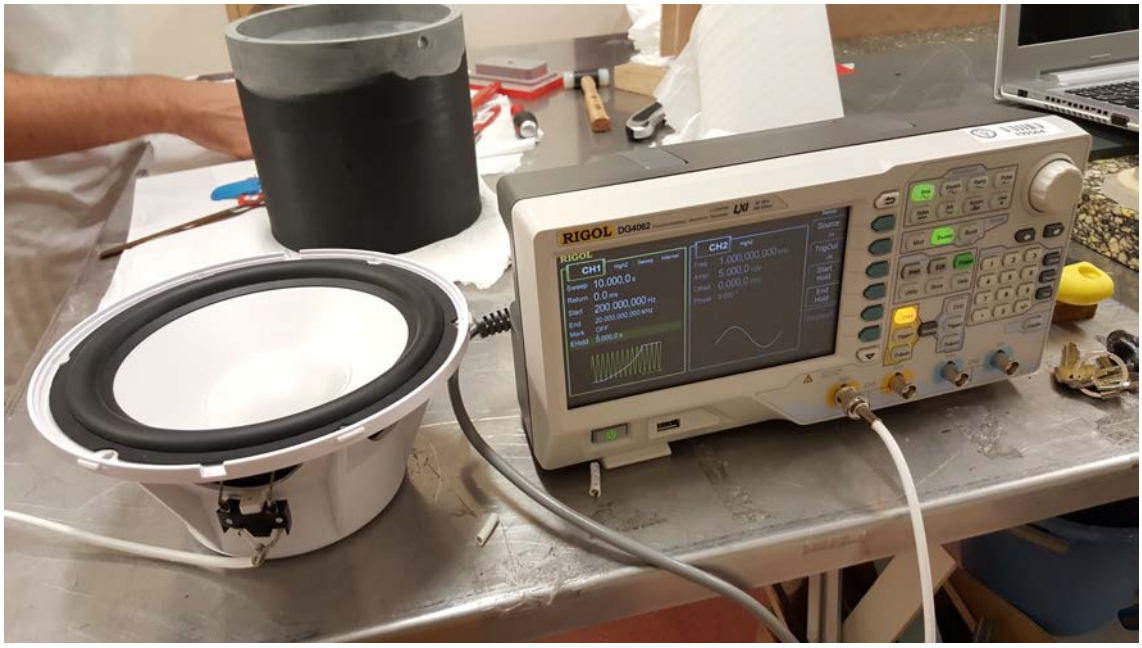

Figure 17: PLMRW8 preliminar performance test

Table 1: Instruments

Device	**Model**	**Characteristic data**
Sensor	Senflex © 93111	Hot-film MEMS
Microphone	POW-1644L-LWC50-B-R	Omnidirectional,50-16000Hz
Loudspeaker	Pyle PLMRW8 Passive	40-18000 Hz, 200 W
Signal generator	Rigol DG4062	2 channels, Up to 200 MHz,50 W

3.3 PWT design

Two are the main geometries that are commonly used in the design of plane wave tubes: square cross sectional and circle cross sectional. To make easier the access to the sample, the cross section was decided to be a square.

At the start of the design of the tube, it was required to have the widest possible frequency range in order to have a clearer frequency response and to be more versatile for possible future experiments. Using reference measures from literature and that the sound speed in water media at 20 degrees Celsius is $c = 1481m/s$, it was proposed a 2,5 m long and 40 x 40 mm section tube that according to Equations 21 and 22 it worked in the range of 148,1 to 18512,5 Hz. This size is commonly used in professional research institutes, although sometimes even larger versions of the tubes are used which are placed vertically in very tall laboratories. However, the scarce of available micro waterproof speakers that would fit in that section -the area of the driver should be at least 2/3 of the cross section of the tube according to the standards [17] [18]- with a suitable frequency response and the inability to perform the experiment vertically made this first model to be discarded.

The section of the tube was modified to 60 x 60 mm and the total length to 1,5 m for easier handling. Moreover it was decided to perform the experiment with the PWT parallel to the ground for handling convenience. To eliminate as far as possible the possible high order vibrational modes and make sure that only plane waves are measured in the sensor, the decided raw material for the tube structure was stainless steel in first place. Although, stainless steel presents high Young modulus, durability and resistance to oxidation in water media, the extremely high cost of the stainless steel and the subsequent limited geometries lead to the decision of making the PWT of PVC. Stainless steel providers only offered very specific cross sections that did not fit the requirements of the regulations in terms of minimum thickness. Moreover, whatever possible machining process necessary would have become way more complex using stainless steel rather than PVC.

Using PVC as raw material enabled the possibility of customizing the PWT completely. Finally the cross section was set to be a 50x50 mm square. This fact added to the length was set to 1,5 meters, according to the expressions 21 and 22 theoretically define the frequency range between 246,83 and 14810 Hz. The PWT was split in four faces that assemble in one another due to the inability for the PVC supplier to create the tube directly. Schematics of the design of the tube are shown in Figures 18, 19 and 20. The final dimensions of the two parts that form the tube are present in Appendix B: Dimensions.

It is highlighted that the manufacturer did not build the tube with the exact dimensions. This fact implied the redesign of the 3D modeled parts and fittings discussed below.

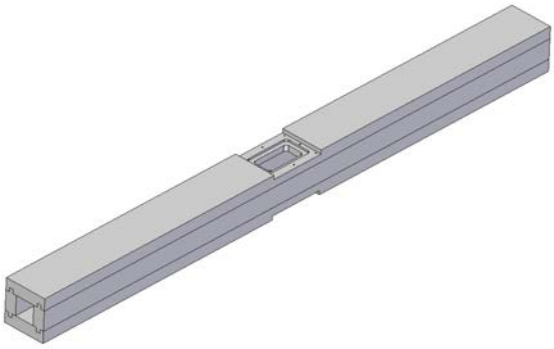

Figure 18: Picture of the PWT

Figure 19: Render image of the PWT

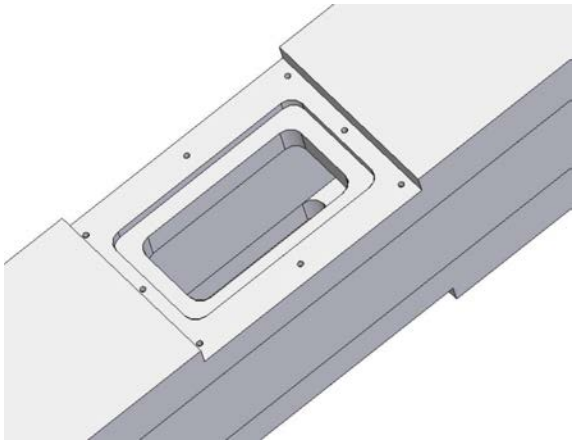

Figure 20: Detail of the PWT

The access to the sample was placed in the middle of the tube as a conservative measure by placing two screwable removable doors. By placing the sample in the middle of the tube it is made sure that the perturbation will be very close to plane wave shape without being affected by possible residual reflections or standing waves. Both the screwable doors present a stepped shape in order to act as barrier for the possible water leakages. Schematics of the microphone door are shown in Figure 21. In addition, o-rings were needed in order to avoid leakage of water. O-rings are rubber bands commonly used in applications involving structures exposed to fluids in order to prevent fluid losses. As O-rings are sold in specific dimensions and geometries, the one used in the experiment was manufactured in the workshop to fit the specific geometry of the door. The doors were 3-D printed using PolyLactic Acid (PLA) as raw material. PLA is a biodegradable polymer that is commonly used in 3D printing applications. In comparison with other supplies as ABS, PLA presents poorer mechanical properties but requires less restrictions and care for the printing process so for the experiment it was more convenient. The 3D printed version of the microphone door is shown in Figure 22. To fit the microphone into the microphone door was not an easy task neither. Regulations impose strict constraints of flush mounting. A very strong adhesive to avoid leakage to the non waterproof parts was

needed. This combination of strict mounting and strong adhesive lead to misplacement of the microphone into the door twice, leading to microphone breakdown.

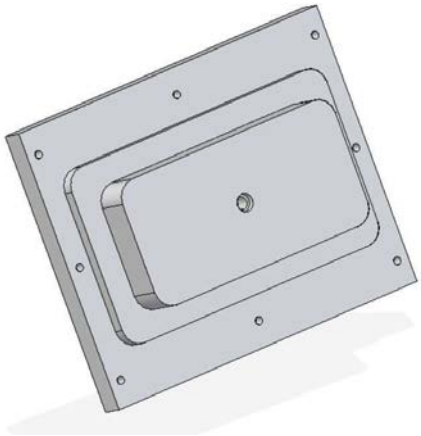

Figure 21: Schematics of the microphone door

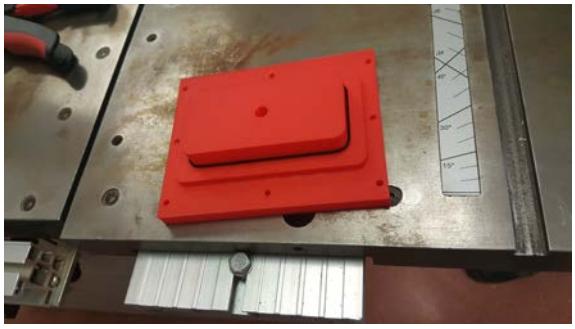

Figure 22: 3-D printed microphone door

In comparison to the microphone door, the sensor door was slightly different. Instead of having an outer planar side, it presents a cavity as shown in Figures 23, 24 and 25. As this experiment has as objective to calibrate sensors to be used in other applications it is required to safely remove the sensor without any damage. For that purpose, into the cavity, paste gum is placed to along with protecting the electronics from any water leakage, to safely remove the sensor. Dimensions of both the sensor and microphone door are shown in Appendix B: Dimensions.

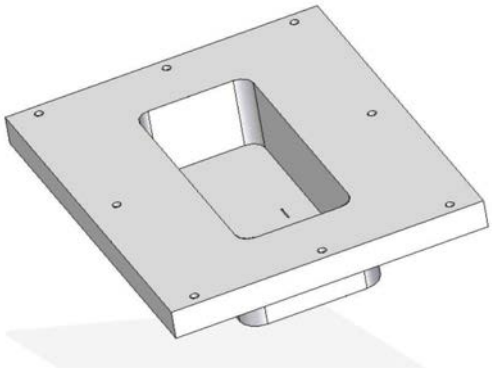

Figure 23: Schematics of the sensor door

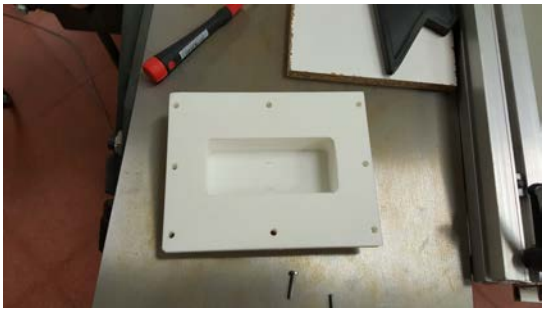

Figure 24: Upper side of the sensor door

Figure 25: Lower side of the sensor door

Once the tube was received and both the doors were printed some machining was needed as the printer and the manufacturers do not work with the same tolerances. According to Carlos Cobos, after analyzing the conditions for the experiment a M3 thread was needed in order to have a strong fixing and zero water leakage. Consequently, it was needed to perform threading process in the tube in order to fix the screwable doors to the main structure of the tube. With the aid of Carlos Cobos the tube was transported to the workshop and post-machined.

Figure 26: PWT in the drilling machine

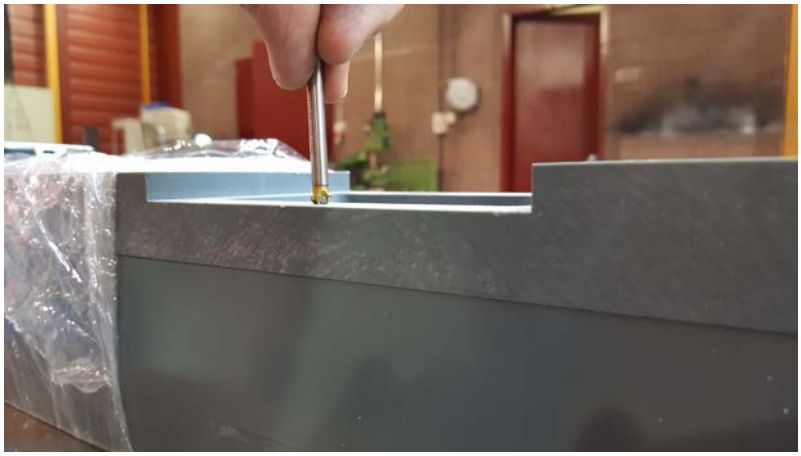

Figure 27: Countersinking process

First, as it was visible that there were some manufacturing errors in the tube, it was required to make sure of the dimensions of the holes in the PWT. The tube was placed in the drilling machine where it was checked that the holes were actually correctly designed as shown in Figure 26. The tube was moved to the work bench in which a countersinking process was carried out in order to facilitate the threading as sketched in Figure 27. A stainless steel HELICOIL© thread insert was decided to be used in order to make sure the requirements of stresses were fulfilled. With the aid of the threading tool the 16 holes were threaded as shown in Figures 28 and 29.

Later, it was needed to widen the diameters of the 3D printed doors with the aid of the removal drill tip. As the 3D printer uses liquid polymers to produce the parts, when the plastic solidifies, it contracts in a different rate in different regions of the part. This fact enables the appearance of thermal stresses which may cause dimensions variations with respect to the original model as well as a detriment on mechanical properties in specific zones of the printed part in this case deformation and reduction of the holes. With the hole widening, the fixing threading action of the M3 screws was improved as the clearance between the doors and the M3 screws was increased. This process is visually described in Figure 30.

Figure 28: Threading process

Figure 29: Threading process complete

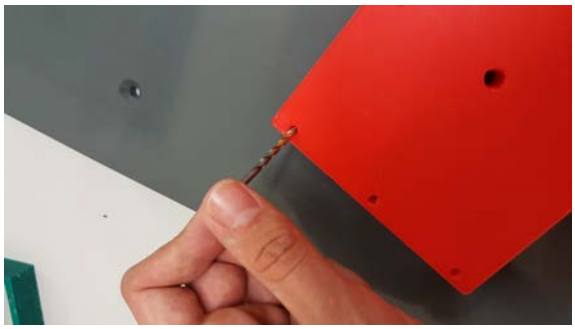

Figure 30: Process of increasing the holes with the aid of a drill tip

To adjust the loudspeaker to the frontal face of the tube fitting was needed. Two fittings were proposed: an exponential decrease, and a circle to square transition.

According to horn theory the exponential fitting was more prone to success due to this geometry allows a smooth change in cross sectional area $S(x)$ and thus in flow properties avoiding wave reflections [24]. The cross sectional area change follows the relationship:

$$S(x) = S(L)e^{-mx} \tag{24}$$

One of many preliminary designs of the exponential fitting is shown in Figure 32. Some modifications were to be done due to the lack of specific dimensions of the tube suppliers and because of the limited domain of the 3D printer at the moment. The model was "Ultimaker^2 extended +" and it required hairspray in order to have good adhesion between the bed plate and the polymer deposed on it. In this way the warping effect caused by the temperature variation between the extruded polymer and the bed is eliminated. The printer is shown in Figure 31. A smaller version of the loudspeaker was suggested and the dimensions of the tube were changed to the ones available in the market 50x50 mm. The fitting was split in four parts which assemble each other carefully avoiding leakages as shown in Figure 33.

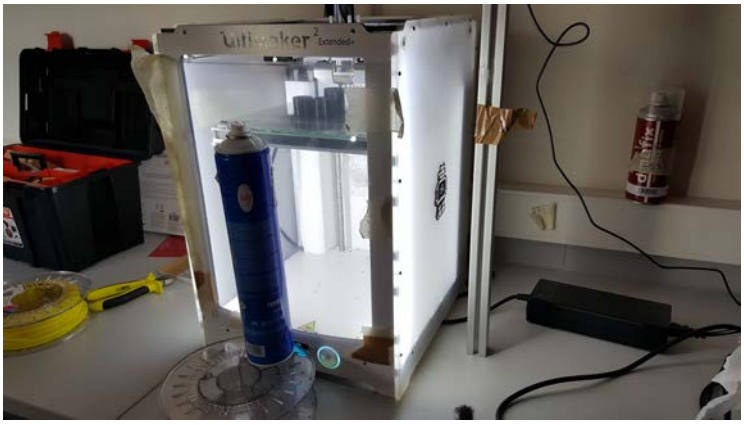

Figure 31: "Ultimaker^2 extended +" 3D printer next to the hairspray

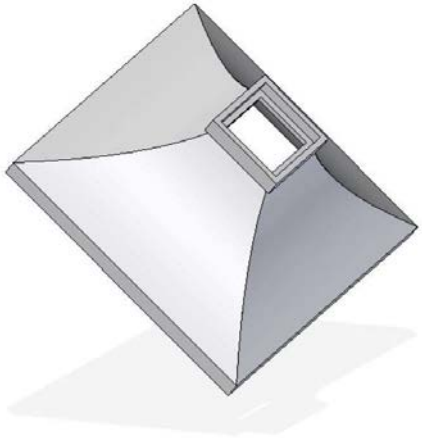

Figure 32: A preliminary design of the exponential fitting

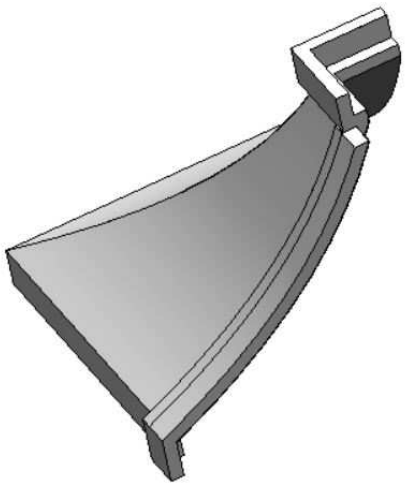

Figure 33: Section of the exponential fitting

Nevertheless, when the loudspeaker was received, it was discussed that because of the specific geometry of the driver, it was more convenient to use finally the design a circle to square transition. The exponential fitting design was discarded, above all, because the printer could not account for that degree of complexity. Moreover, if the part was split in four parts the risk of water leakage was excessive. This radical change in design would provide better drive fixing avoiding any water leakage. Moreover, this new version includes an additional tube to fill and drain the water from the tube. This tube is designed according to hydrostatic principles in order to make sure the tube is completely filled. Schematics of the fitting are shown in Figures 34 and 35. The "Raise3D Pro 2 Plus" 3D printer was received increasing the printing domain significantly and avoiding splitting the part in order to be printed. Again, there was needed to account for the thermal stresses, in this case the optimum way to deal with dimension changes was decided to print only a critical section of the part leading to time, material and therefore cost reduction. The critical parts were obviously the joints with the loudspeaker and the main tube structure. Rather difficult was the case of the joint with the loudspeaker. This was because the position of the inserts of the loudspeaker did not enable a lot of margin to perfectly design the grooves of the fitting. However, when the final printing process was being performed, due to the excessive weight of the part, polymer supply run out. Usually when the polymer is still at high temperature is not a problem, but when this occurred there was nobody to replace the PLA roll. When the printing process was resumed, due to the difference in temperature adhesion failures lead to part rejection. To avoid future possible failures, weight and complexity reduction of the part was needed. By keeping the same critical dimensions (length, diameters etc), solid walls were replaced by a net of cells. The filling tube was removed and a external cylindrical cover was designed. In this way the weight of the part plus the draw (substrate in which the part is printed) decreased drastically solving the problem. The printing process is shown in Figure 37. Schematics and dimensions of this design are shown in Figures 36 and 38 and Appendix B: Dimensions respectively, notice that the cells are not shown in the drawing planes because of simplicity. Again, similarly to the case of the 3D printed doors, to fix the loudspeaker to the fitting, 6 M3 threads were used to assure a nice stable configuration.

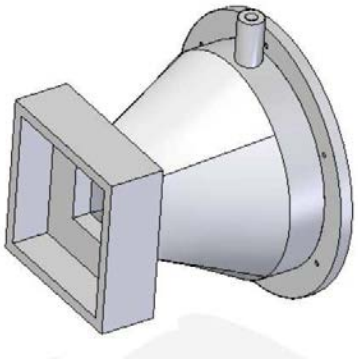

Figure 34: Front view of the fitting

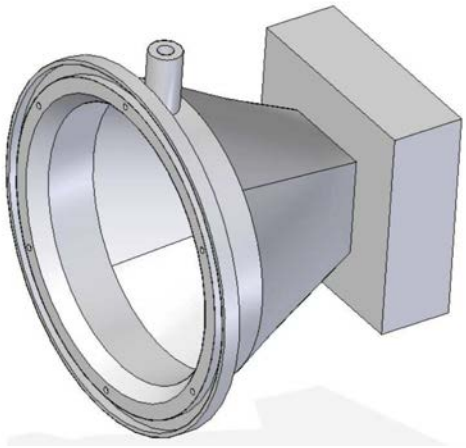

Figure 35: Rear view of the fitting

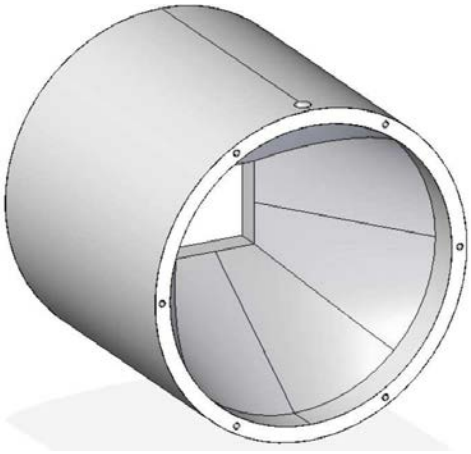

Figure 36: Final fitting design

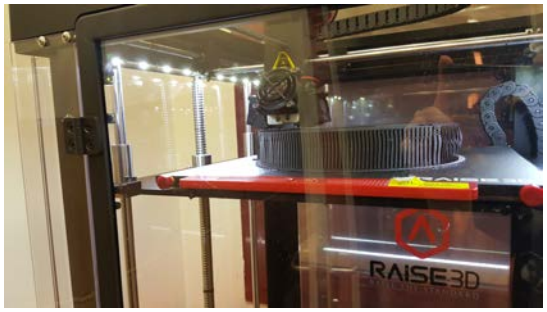

Figure 37: Fitting being printed

Finally, a back plate was designed with a specific geometry in order to avoid water leakages to the exterior. The printing process is shown in Figure 39, note that thanks to the "Raise 3D" printer parameters as the extruder and bed temperatures can be monitored at any time, so better part printing quality is assured. Schematics of the back plate are shown in Figure 40. Dimensions of the back plate are shown in Appendix B: Dimensions.

Figure 38: Final fitting printed

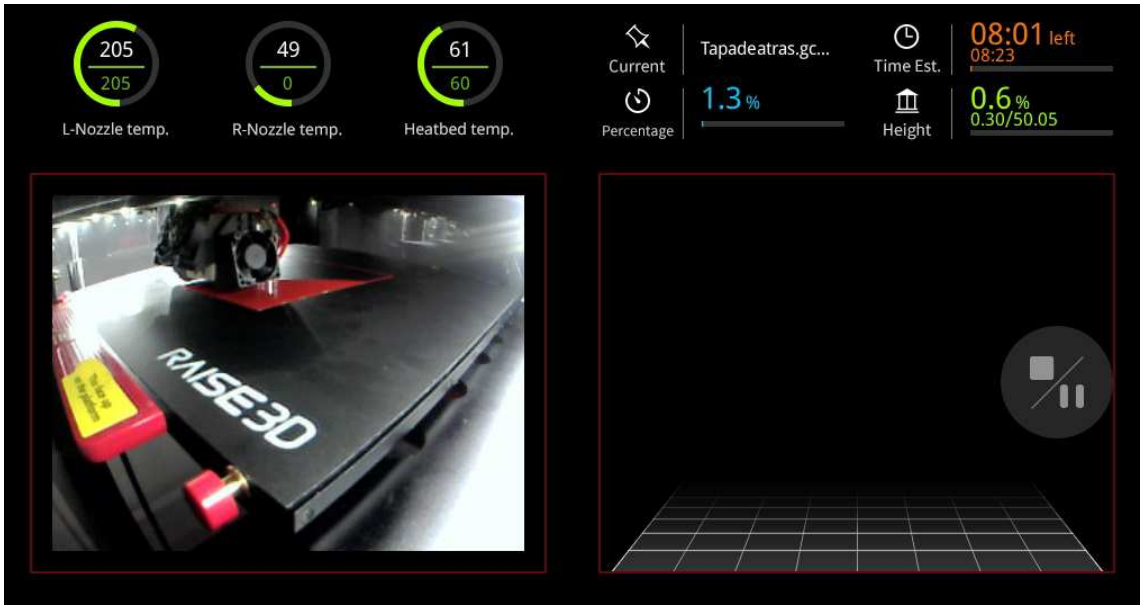

Figure 39: Rear plate being printed

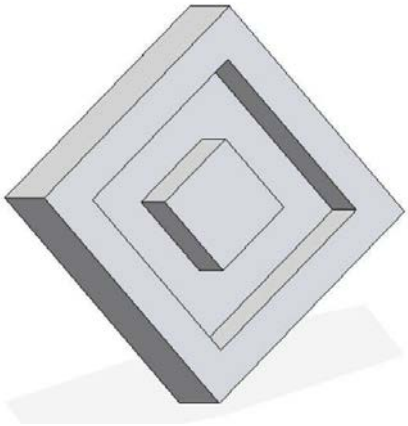

Figure 40: Schematics of the rear plate

As the tube is finite, the sound waves that propagate through the tube will impact with the rear plate and will be reflected backwards. This reflected wave although it will lose some of the energy, it will encounter the incoming propagating wave and will form a standing wave that obviously will perturb the measurements. As recommended by different authors [25] [13] a wedge shaped polyurethane foam should be used to mitigate the effect. Although it is stated that the choice of the geometry of the foam is shown to be not relevant at first instance, the wedge shape is chosen to maximize the surface reflection area in the direction convenient for the experiment. An angle of 45 degrees is taken in order to decrease the costs -as it is the most typical in stores- and manufacturing issues. The wedge should be glued with silicon to the inner side of the rear plate. It was decided to use the CHOVA acoustic foam, shown in Figure 41, due to it is relationship between properties and cost.

Due to the fact that the experiment was to be performed in the water media, it was needed to test the adhesive properties of the silicone by submerging in water some foam glued to the rear plate as shown in Figure 42. The adhesion test was proved to be a success. The final appearance of the rear plate assembly is shown in Figure 43.

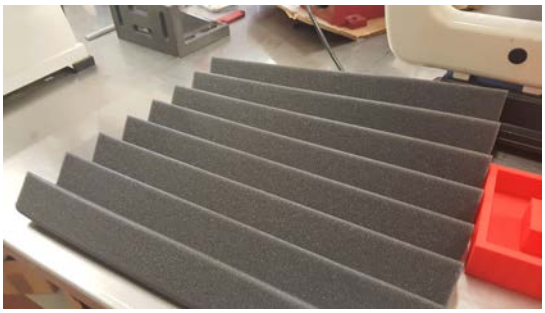

Figure 41: Chova wedge shaped acoustic foam

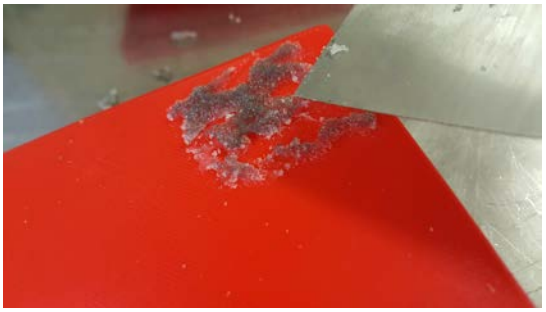

Figure 42: Adhesion test

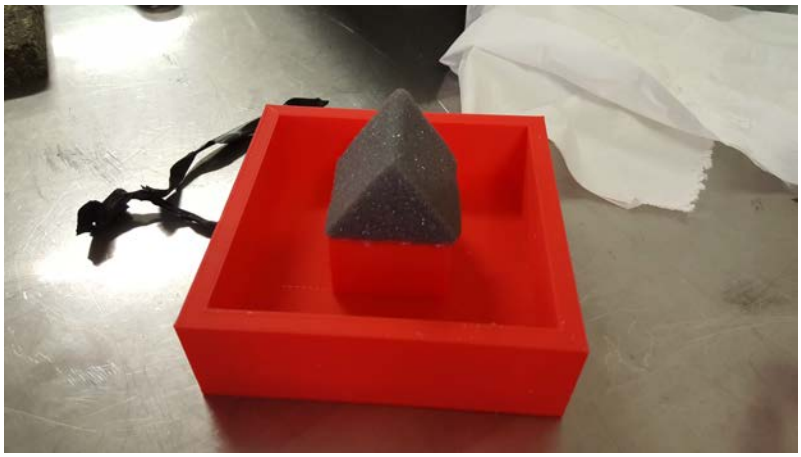

Figure 43: Final rear plate assembly

Finally when the all the parts were ready, an additional preliminary test was needed. The tube was placed vertically and water was poured in order to see if there was some water leakage. As Carlos Cobos foreshadowed, the 3D printed parts were not waterproof. As they are made of superimposed polymer filaments, water can move through the space between the filaments. The solution was to coat each part with a sealing paint, generating a protective film avoiding leakages. The application process of the sealant is shown in Figures 44. As the printed parts present a porous behaviour several coating layers were needed to be provided each 24 hours. For instance the final coated version of the fitting is shown in Figure 45.

When the waterproof properties of the parts were tested, the rear plate was already pasted with silicone to the main structure. Therefore to properly paint the part, part destruction was needed. The rear plate was printed again, coated several times and after the foam wedge placement it was glued to the main structure.

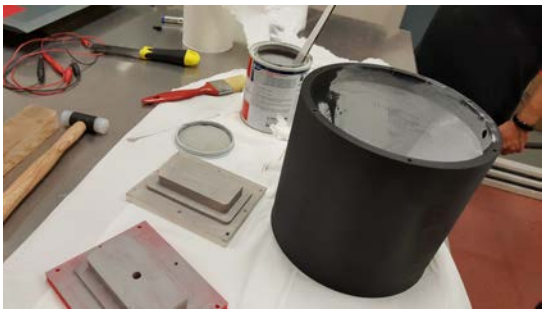

Figure 44: Coating process

Figure 45: Fitting completely coated

Lastly, according to Carlos Sanmiguel to avoid interference and wave reflection problems an acoustic foam cover in the inner side of the fitting was needed. The manufacturing process of the foam layers is shown in Figure 46. These layers were carefully pasted to the fitting expansion cavity with silicone as seen in Figure 47. The final result is shown in Figure 48.

Figure 46: Foam cover

Figure 47: Foam adhesion

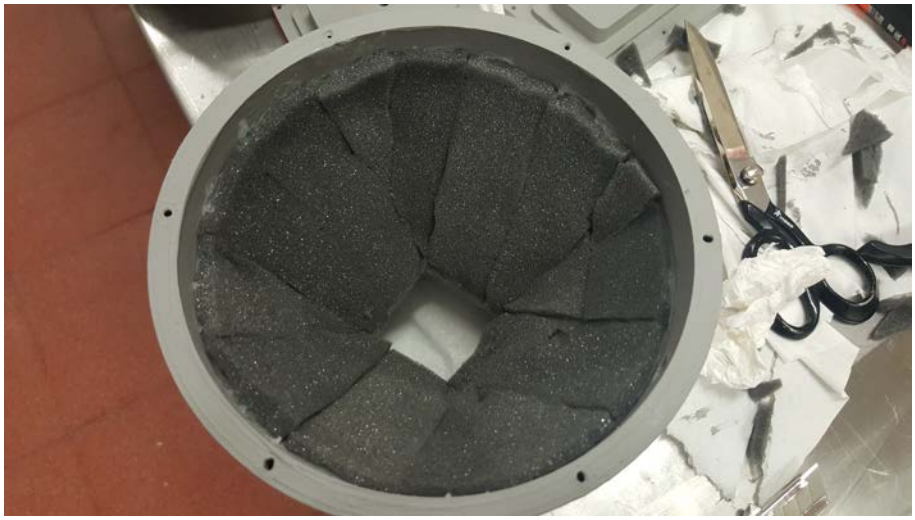

Figure 48: Final fitting covered with foam

4 Conclusions

Fluid mechanic measurements are a incredibly tough task, the fact that many of the processes do not occur visible to the human eye force to rely on signal instrumentation. Experimental hydrodynamics has concluded to be a complex mixture of physics, electronics and manufacturing that has to work as whole understanding the limitations of each other. The fact that the most topics covered in this thesis are not so familiar to an aerospace engineer was also critical and tough. Above all, the electronics part, has supposed a challenge. To deal with complex electrical designs even for electrical engineers themselves without a strong background on the topic has implied extra efforts. To work with electrical apparatus means to introduce new sources of uncertainties and errors that should be accounted for. A good understanding of the limitations an operating regimes of the devices is key to obtain good and reliable results.

Moreover, it has been understood how real engineering projects are. To be able to take part in all the different stages of a project has increased the knowledge in project management topics. It has been proved that no step is straightforward and ultimate. Every single little stage of the project can be subjected to changes and reformulations. Each decision has each own process of confirmation. An idea comes, feasibility is discussed, cost is estimated and drawbacks are foreseen. When the idea/concept is approved, the project can continue. Schedule times vary quite much with respect to the ideal ones. This is the main reason for which this thesis requires further continuation and set the basis to further work. As it was seen during the previous section, every time a step was achieved, different problems that were previously unknown at first appear. And again they have their own process of fixing. Hypothesis are proposed and possible solutions are derived. Sometimes extra tools or components are needed. These have to be budgeted, purchased and received what increases the time spent and consequently costs. Just to enumerate some problems that exemplify this statement: tolerance adjustment, extra machining, electronic failures (transistors or jack connections), microphone membrane damage, printing failures, delivery times, bureaucratic issues etc. One of the most annoying -if not the most annoying- things through the project development is the fact that in real processes every supplier works with its own range of tolerances if not specified. In this project the tolerances of the tube were not given to the manufacturer because strict tolerances can multiply the cost of the device. This fact implied that these little changes were needed to be measured and taken into account for the 3D printing designs that indeed had its own error range due to thermal stresses. In this line, 3D printing has been conclude to be a good candidate for future manufacturing but it is still currently troublesome. Without the required knowledge it is easy to obtain defective parts because there are a lot of parameters such extruder control or adhesion issues that require high supervision.

It is interesting to remark that workshop issues are very important. Sometimes although a concept project is approved, to deal with it in the workshop is different. There are things that theoretically can be performed but in reality they cannot such 3D printing part with a complex design or performing a threading process in a very thin wall. By having worked at the workshop level, further insight on the topic

has being acquired, so for other projects better manufacturing and maintenance considerations will facilitate workshop workers task. Finally, in general, to work with water has supposed extra care. To isolate electronic components from the fluid has supposed extra effort and costs. Coatings, o-rings and hydrostatic pressures were need to be taken into account. Above all, it is needed to be taken into account that this calibration method of the sensor has only been proved in air media. This analysis probably has not been performed before what makes the calibration process even more challenging.

5 Recommendations and further work

As this is a large research project, some recommendations based on empirical and rational knowledge are provided in order to help future researchers. First some guidelines of the next steps are proposed and finally some general considerations are given.

- First, a serious calibration of the microphone and the loudspeaker should be performed. By doing a frequency sweep analysis and comparing the results with the ones of the datasheets included in Appendix C: Datasheets the proper response of the devices should be checked. To test the measurement system, a preliminary experiment with the microphone and the loudspeaker should be performed. It is a simplified version of the experiment in which there is no tube and the media is air. The recommended set-up is shown in Figure 49. In the anechoic chamber, the loudspeaker is recommended to be placed at 10 centimeters from the microphone as perfectly aligned as possible to assure the less acoustic energy dissipation as possible. The microphone should be connected to the laptop with the same circuit as the one of the preliminary test Figure 11. A frequency sweep would be generated in the RIGOL DG4062 such the whole range of frequencies is covered. According to the limitations of the signal generator different test are proposed in Table 2. Data should be carefully checked because "Matlab" digitalize the data so no further conclusions about amplitude magnitude could be derived. Using the sensitivity frequency response of the microphone and loudspeaker the signals can be compared looking for convergence.

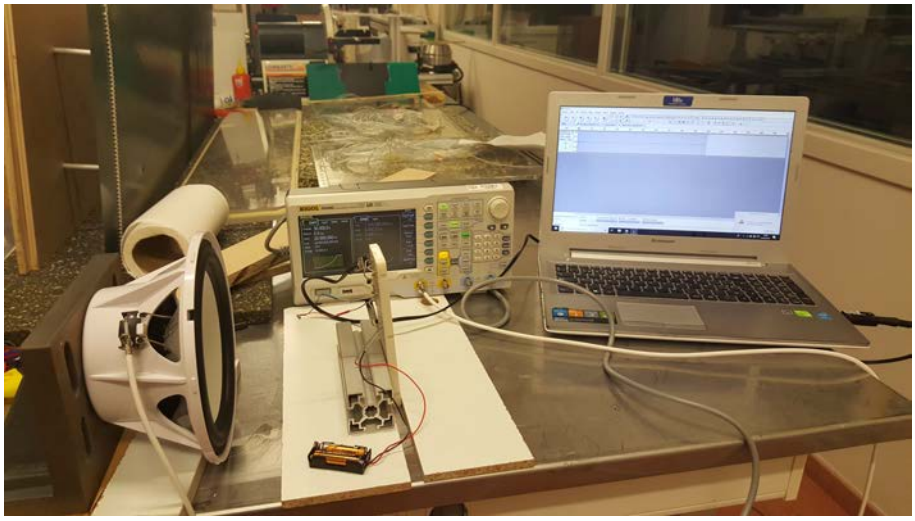

Figure 49: Suggested set-up

- Similarly, the tube frequency analysis of the tube in air media should be carried out. This would enable the characterization of the natural frequencies of the PWT what will be helpful for drawing conclusions in the final calibration. For that purpose, again a frequency sweep approach would be necessary. The

Table 2: Recommended tests

Amp.[V]	**Low freq.[Hz]**	**High freq.[Hz]**	**Time[s]**	**Type**	**Hold[s]**
10	20	20000	30	Linear	5
10	20	20000	30	Logarithmic	5
10	20	20000	100	Linear	10
10	20	20000	100	Logarithmic	10
10	20	20000	300	Linear	10
10	20	20000	300	Logarithmic	10

loudspeaker should be attached to the fitting and this latter to the main tube. The microphone door (with the microphone properly placed) would be screwed to the main tube structure. The electronic microphone connections are the same as the ones of the first experiment. The sensor door is to be put in place but with the sensor orifices blocked. Again with the aid of the RIGOL DG4062, frequency sweeps with similar parameters like the ones of Table 2 would be performed. When deviations from the frequency response of the microphone appear resonance might be present. The tests should be bounded little by little in the observed range of critical frequencies so an accurate resonant frequency could be derived. After this, the same procedure in water media should be performed as the calibration will take place in the water environment.

- According to the manufacturer the maximum current that the sensor can withstand is dependant on the substrate and the media in which the sensor works. This is of course due to the heat transfer issues. Convection due to the heat flow from the sensor to the media and conduction due to the one from the sensor to the wall. So before the experiment takes place, some initial estimations should be done in order for the sensor not to be damaged. The sensor should be tuned with the hot-wire box available in the university so the current does not damage the sensor. Probably, the sensor will operate in CTA mode so the overheat ratio should be estimated. Collaboration with the electronics department is strongly advised due to the high sensitivity of the hot-film sensor.

- Hot-film calibration in air goes next. Although, calibration in air is not the main aim of the project, research on the topic will make some problems appear what should be dealt with. In addition, air calibration is easier than the water one because of previous references. Dividing the complex calibration problem in simple steps will for sure simplify the difficulty. The experiment as previously stated implies the whole assembly of the loudspeaker, fitting, tube, the two doors, the sensor and the microphone. The way in which it should be performed is the same as the experiment of section. A frequency sweep is generated that will induce an oscillatory boundary layer that will induce a shear stress at the wall. Using the formulas from the state of the art section, a matching result should be obtained between theoretical results and experiment. With the aid of the results of the tube frequency response previously derived conclusions could be drawn.

- Finally the calibration in water media should take place. It is estimated that perhaps some leakages may occur because water coating is not perfect but it should not affect quite much the results. Similarly, the data for the water frequency analysis would be used to understand better the results. It is recommended to carefully check the quality of the water in order it to be as pure as possible. Metallic ions or dirt deposition in the sensor might change the frequency response. Bubble formation avoidance should be taken into consideration as well because bubbles might alter the thermal distribution around the sensor leading to incorrect readings.

Additionally some general recommendations for the future experiments are provided:

- It is suggested to use a microphone amplifier in order to have less recording issues. With the current microphone, high amplitude acoustic waves are needed in order to be sensed by the microphone.

- Perform the tests in a place with the least electrical noise possible. Magnetic fields can introduce modifications in the measurements of the sensor and microphone. If not possible, a Faraday cell should be manufactured to isolate the device.

- Repeatability of the tests. It is strongly recommended to perform the calibration several times before drawing any strong conclusion. Some procedures should be described prior testing in order to minimize the time spent assuring the best safety and quality conditions. A general test protocol is provided in Appendix D: Test protocol.

- There are a lot of parameters which probably have influenced this project. It is recommended to try to reproduce the tests changing some of them to study the sensitivity of the results to that particular parameter variation. As an example the geometry of the foam at the end of the tube can be taken into consideration. Although wave reflection was tried to be minimized, imperfections may change the results.

- To achieve higher printing quality use ABS instead of PLA, that will imply probably some slight modifications in the design of the parts and more dedication and care during the printing process.

6 Project planning

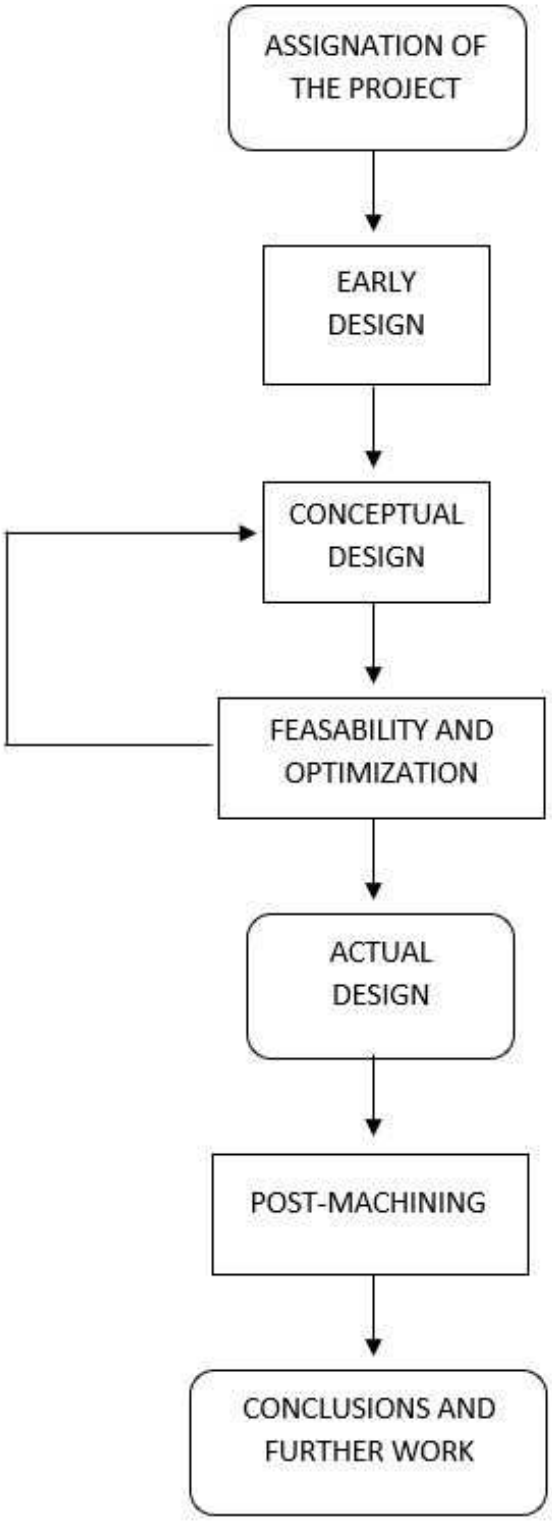

Figure 50: Process planning flowchart

A graphical representation of the project plan is shown in Figure 50. The different steps followed to the project completion are described below:

- **Assignation of the project**: Due to the intrinsic preferences of the student to know more about fluid mechanics and turbulent flow adding to the fact of experience real contact with the workshop and the laboratory environment, the project was chosen by the student.

- **Early research**: During the first months, research process started. It was needed to improve and expand the student background in turbulence, boundary layer and experimental fluid mechanics. Loads of papers about PWT were studied, to understand many concepts it was needed to research many topics on generation, propagation and reflection of waves. Moreover the electronics market was explored to have an early approach of the costs.

- **Conceptual designs**: The next months involved the gross work load of the project. The student elaborated loads of preliminary PWT designs that were finally discarded. Lots of regulation papers were explored involving PWT design and manipulation. The student took direct contact with several raw material suppliers to estimate at a greater extent the budget of the project.

- **Feasibility and optimization**: As previously stated, the design of the PWT was a dynamic process in which the modification of a single component involved the change in many others. Adding to this fact, cost were optimized whenever was possible as it was the case of choosing PVC instead of stainless steel as raw material, or to use a simple condenser microphone instead of a expensive hydrophone. The acquisition of the new 3-D printer supposed also some changes in the fitting design.

- **Actual design**: The final design was established. The student made final contact with the supplier to formalize the order and specify the format for the receipt paperwork process. Final material costs were performed. The loudspeaker and the microphone were carefully tested, to fulfill this aim research on electronics was required. The different parts were finally printed and its waterproof properties checked.

- **Post-machining**: Due to several small failures in the manufacturing process, some grinding was required. Moreover the threading process was performed in the workshop. Coating of the printed parts was carried out. Different adhesion failures were reported and lead to microphone replacements.

- **Conclusions and further work**: Once the design and manufacturing process was finished, some conclusions could be drawn as well as an analysis of the way of how the experiment could be optimized and improved was performed. Moreover some guidelines to continue with the research were provided. The final budgets with the amortization expenses and electricity and salary costs were elaborated. The test protocol was carefully designed in order to provide some guidance for the future.

References

[1] Richard Feynman. *The Feynman Lectures on Physics Vol 1.* 2005.

[2] Edward. N Lorenz. "Deterministic Nonperiodic flow". In: (1963).

[3] William K. George. *Lectures in Turbulence for the 21st Century.* 2013.

[4] Hassan M. Nagib Peter A. Monkewitz. "How comparable are the three "canonical" turbulent flows ?" In: *XXIV ICTAM* (2016).

[5] *Impuesto sobre Sociedades.* Standard. Avenida de Manoteras, 54,28050 MADRID: BOLETÍN OFICIAL DEL ESTADO, 2018.

[6] Ludwig Prandtl. "Über Flüssigkeitsbewegung bei sehr kleiner Reibung". In: (1904).

[7] Stephen B. Pope. *Turbulent flows.*

[8] William K. George. *Lectures in Turbulence for the 21st Century.* 2013.

[9] A.N Kolmogorov. "The Local Structure of Turbulence in Incompressible Viscous Fluid for Very Large Reynolds numbers". In: (1941).

[10] M. Sheplak V. Chandrasekaran L. N. Cattafesta. "Dynamic calibration technique for thermal shear-stress sensors with mean flow". In: (2005).

[11] Andrew F. Seybert. "Notes on Absorption and Impedance Measurements". In: ().

[12] S. Breuer Mark Sheplak Aravind Padmanabhan. "Dynamic Calibration of a Shear-Stress Sensor Using Stokes-Layer Excitation". In: (2001).

[13] Lennart Löfdahl and Mohamed Gad-el-Hak. "MEMS-based pressure and shear stress sensors for turbulent flows". In: (1998).

[14] P J Thomas Wenjie Wang and Tongqing Wang. "A frequency-response-based method of sound velocity measurement in an impedance tube". In: (2017).

[15] Gerald A. Sabin. "Acoustic-Impedance Measurements at High Hydrostatic Pressures". In: (1966).

[16] Ronald A. Roy Preston S. Wilson and William M. Carey. "An improved water-filled impedance tube". In: (2003).

[17] *Acoustics — Determination of sound absorption coefficient and impedance in impedance tubes.* Standard. Genève, Switzerland: International Organization for Standardization, 1998.

[18] *Standard Test Method for Impedance and Absorption of Acoustical Materials Using a Tube, Two Microphones and a Digital Frequency Analysis System.* Standard. West Conshohocken, USA: ASTM.

[19] Scott Sutherland Corbet III. "A two-hydrophone technique for measuring the complex reflectivity of materials in water-filled tubes". In: (1983).

[20] N. Atalla J.F. Allard. *Propagation of sound in porous media.*

[21] Peter D. Dean R.V.Digumarthi. "Use of a water impedance tube to evaluate the performance of a smart skin piston element". In: (1997).

[22] Debra M. Kenney and Peter H. Rogerst. “A Short Water-filled Pulse Tube for the Measurement of the Acoustic Properties of Materials at Low Frequencies”. In: ().

[23] G.J.J. Ruijgrok. *Elements of aviation acoustics*.

[24] John Eargle. *The loudspeaker handbook*.

[25] Carlos Sanmiguel. “Measurements of Pressure Fluctuations in a Turbulent Boundary Layer”. In: (2014).

Appendix A: Budget

In the following section an overall budget is to be developed. Different assumptions should be made as some information is confidential. For the case of salaries, some reference values above the standard ones are taken according to the BOE for this university institution. For the labour cost of student is assumed to be 9€ . For the Web of Science full access license, no information has been obtained so a conservative value of 500€ per year will be assumed, as it provides full access to books and articles. There are also variable costs as for the electricity for which value changes from day to day even from hour to hour, so an average value will be used. Costs can be classified into:

- **Direct material costs**: involve all the raw materials and components directly used in the project development. For the case of the components, amortization is needed to be taken into account. This means that all the cost of a asset should not be taken into account directly, as it presents an operating life larger than the time spent during the project. The way amortization will be taken into account is by using some reference coefficients presented in BOE-A-2014-12328 updated on July 4^{th} 2018 [5]. These coefficients represent percentages of yearly amortization showing how an asset value decreases from year to year. Average month values since the acquisition of the asset are taken because of simplicity. Tables 3 and 4 represent the expenses for raw materials and components respectively. Note that in the total, two more microphone were added because as they were broken all the cost has to be taken into account.

- **Direct labour costs**: are related with the salaries of the workers involved directly in the development of the project. Mainly the student salary is the principal expense although for the proper handling and operation of some tools the technician help was needed during some hours. Table 5 represents the direct labor costs estimation.

- **Indirect manufacturing costs**: involve rent, energy along with the different license costs. For the budget, because of simplicity, only electricity, internet and license cost will be accounted. License costs are included in table 6. Electricity costs are safely estimated by knowing the power consumption of every electric device and the time of usage. The average electricity cost is taken to be 0.12€/KWh. For simplicity it is conservative assumed that always 2 LED bulbs are switch on always. The electricity analysis is shown in Table 7. Finally, internet costs can be computed knowing that the typical rate for optical fiber is 57,95€/month leading to a value of 539,55€ for the whole project time.

- **Indirect labor costs**: include administrative costs, cleaning costs, executive and supervisor salaries. Cleaning costs, administrative costs are assumed to be 3% of the total direct labour costs as no reference values can be extrapolated by any data source. Leading to a total value of 105€.

With all the exposed data the final cost of the project can be computed by

simply adding all the costs previously mentioned. The final total costs are listed in Table 8.

Table 3: Direct raw material

Concept	**Unitary cost [€]**	**Quantity**	**Total [€]**
Acoustic foam	3,8	1	3,8
O-ring roll	3,5 (per meter)	0,6 (meters)	2,1
3D printer polymer	29,99	4	119,96
Tin	5	1	5
Adhesive	6,6	1	6,6
Coating	6,95	1	6,95
TOTAL:			144,41

Table 4: Direct material components

Concept	**Unitary cost[€]**	**Quantity**	**Amortization**	**Life[months]**	**Total[€]**
Sensor	58,54	1	20%	10	9,75
Microphone	3,16	2	20%	1	0,05
Loudspeaker	38,22	1	20%	7	4,45
Tube	624,35	1	25%	5	65,03
Laptop	750	1	25%	9	140,62
3D printer	6048,79	1	20%	5	504,06
Driving circuit	17,3	1	20%	7	2,01
Sound card	6,13	1	20%	7	0,71
Water container	3,99	1	15%	4	0,19
Tin welder	13,95	1	12%	7	0,97
Threads	0,4	22	25%	5	0,91
Screws	0,5	22	25%	5	1,14
Brush	2	1	12%	2	0,04
TOTAL(adding the two microphones):					736,25

Table 5: Direct labor costs

Concept	**Salary [€/hour]**	**Hours**	**Total [€]**
Student	9	360	3240
Technician	13	20	260
TOTAL:			3500

Table 6: License costs

Concept	**Cost [€/month]**
Matlab	6,5
Solid Edge	11,2
Microsoft Office	1,08
Web of Science	41,66
TOTAL (9 months):	543,96

Table 7: Electricity cost

Concept	**Power [W]**	**Hours**	**Total [€]**
2 Bulbs	7	330	0,55
Computer	41	330	1,62
3D Printer	600	168	12,09
Loudspeaker	200	21	0,5
Signal generator	50	21	0,12
Drilling machine	450	0,25	0,01
Welder	35	0,25	≈ 0
TOTAL:			14,89

Table 8: Total costs

Type of cost	**Concept**	**Subtotal [€]**
Direct material	Raw materials	144,41
Direct material	Components	736,25
Direct labor	Direct labor	3500
Indirect labor	Indirect labor	105
Indirect manufacturing	Licenses	543,96
Indirect manufacturing	Electricity	14,89
Indirect manufacturing	Internet	539,55
TOTAL:		5584,06

Appendix B: Dimensions

Revisiones			
Rev	Descripción	Fecha	Aprobado

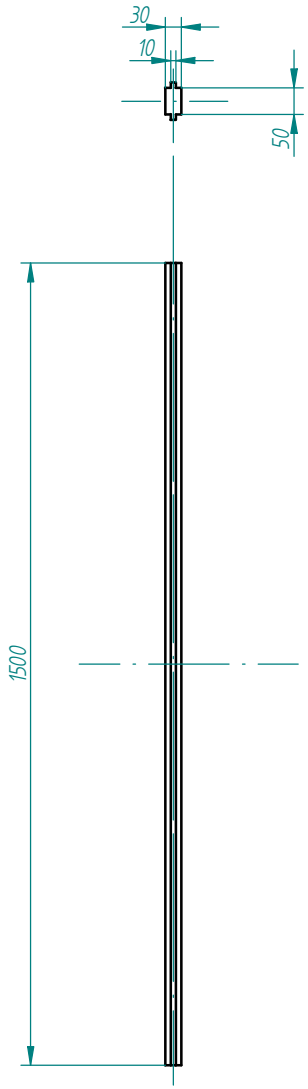

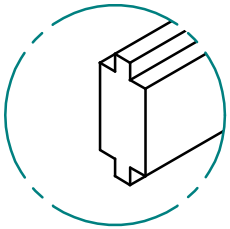

DETALLE A

A

	Nombre	Fecha
Dibujado	Pablo Alejandro	11/04/18
Comprobado		
Aprobado 1		
Aprobado 2		

Salvo indicación contraria
cotas en milímetros
ángulos en grados
tolerancias ±0,5 y ±1°

SOLID EDGE
EDS-PLM SOLUTIONS

Título

A3	Plano	Rev

Archivo: cara_lateral.dft

Escala	Peso	Hoja 1 de 1

Revisiones			
Rev	Descripción	Fecha	Aprobado

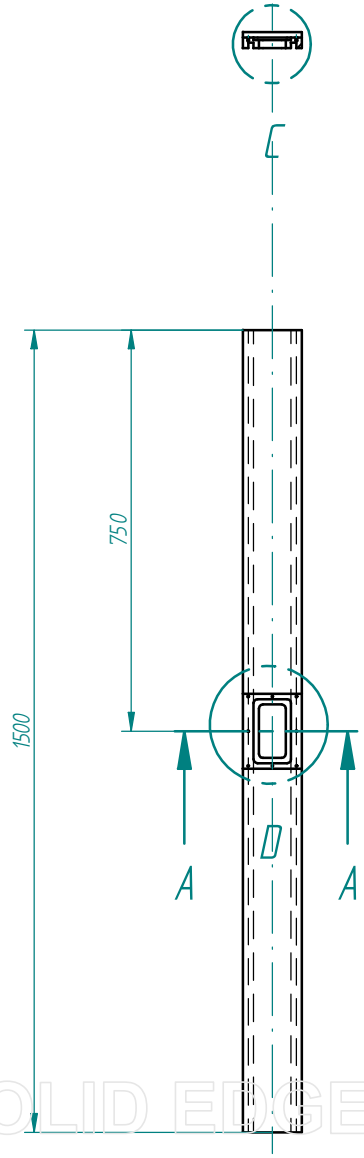

CORTE A-A

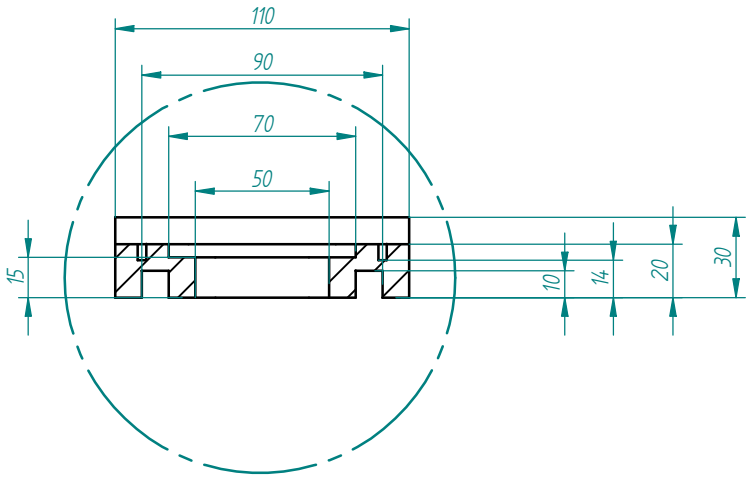

DETALLE C

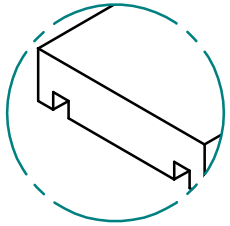

DETALLE B

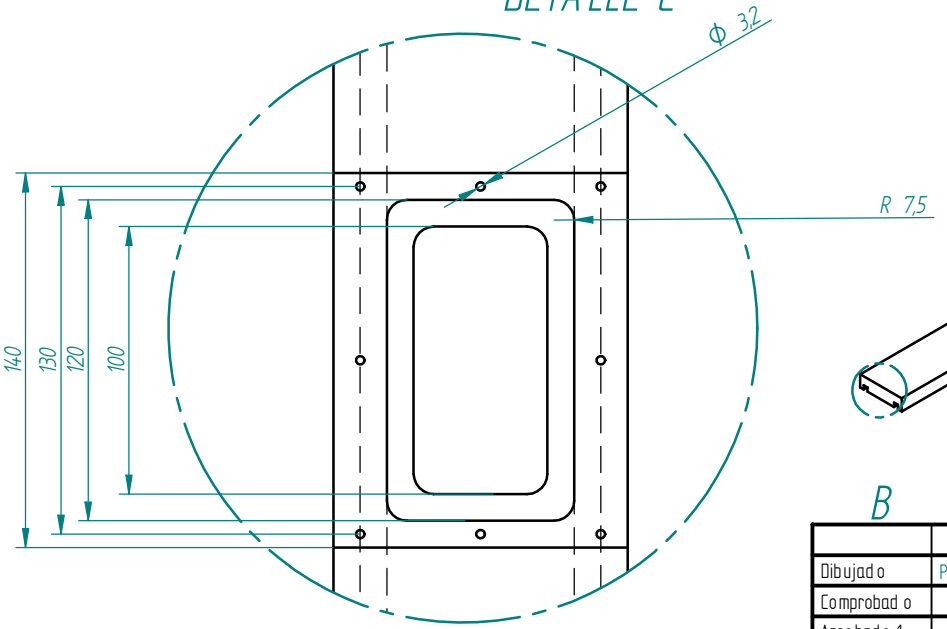

DETALLE D

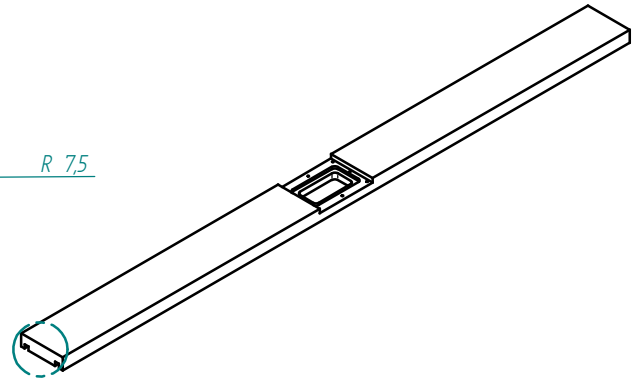

B

	Nombre	Fecha
Dibujado	Pablo Alejandro	11/04/18
Comprobado		
Aprobado 1		
Aprobado 2		

Salvo indicación contraria cotas en milímetros ángulos en grados tolerancias ±0,5 y ±1°

SOLID EDGE
EDS-PLM SOLUTIONS

Título

A3	Plano	Rev

Archivo: corte_superior.dft

Escala	Peso	Hoja 1 de 1

Revisiones			
Rev	Descripción	Fecha	Aprobado

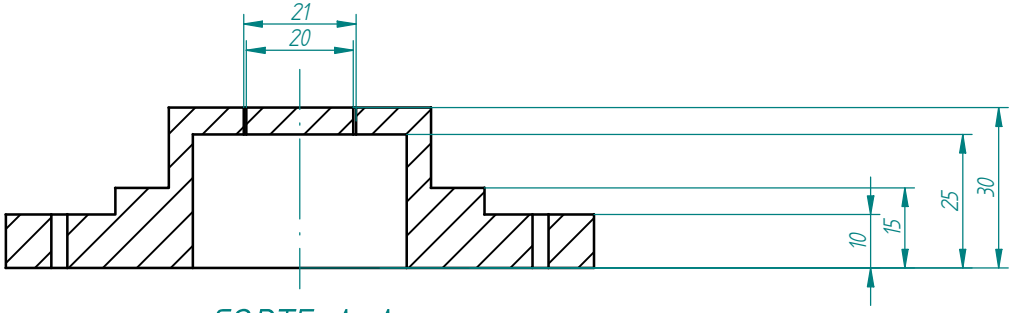

CORTE A-A

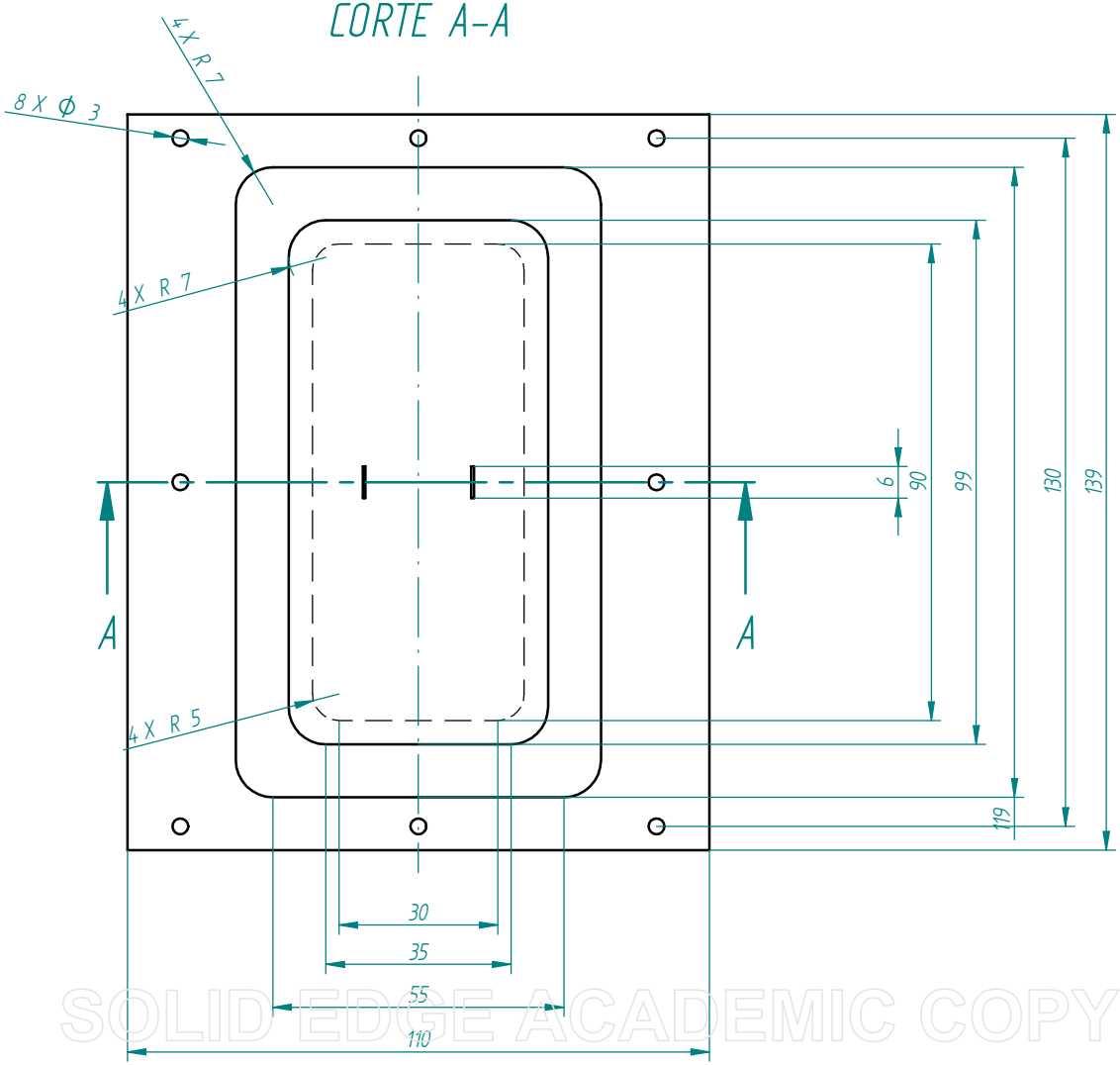

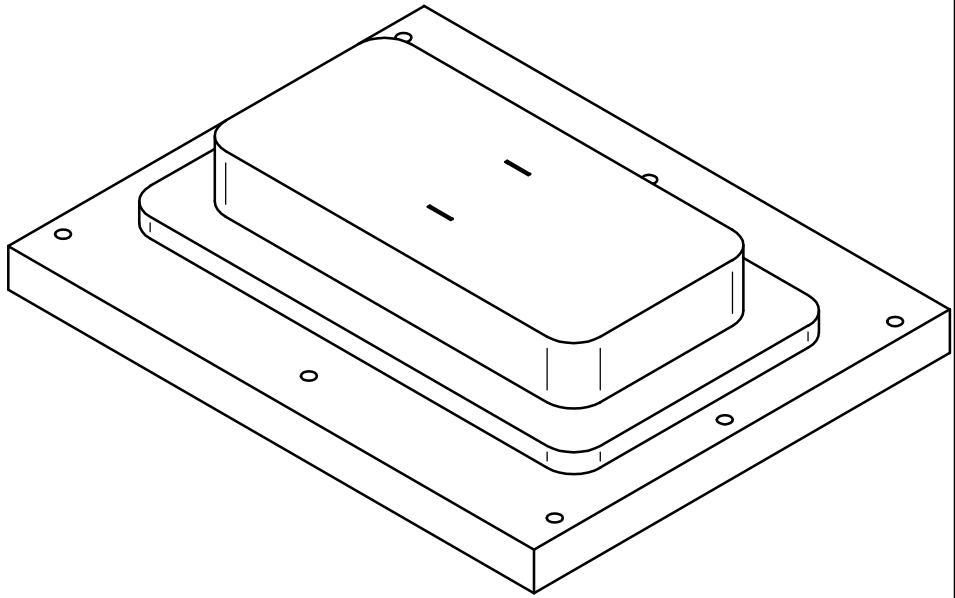

	Nombre	Fecha
Dibujado	Pablo Alejandro	1/01/01
Comprobado		
Aprobado 1		
Aprobado 2		

Salvo indicación contraria cotas en milímetros ángulos en grados tolerancias ±0,5 y ±1°

SOLID EDGE
EDS-PLM SOLUTIONS

Título

A3	Plano	Rev

Archivo: Plano3

Escala	Peso	Hoja 1 de 1

Revisiones			
Rev	Descripción	Fecha	Aprobado

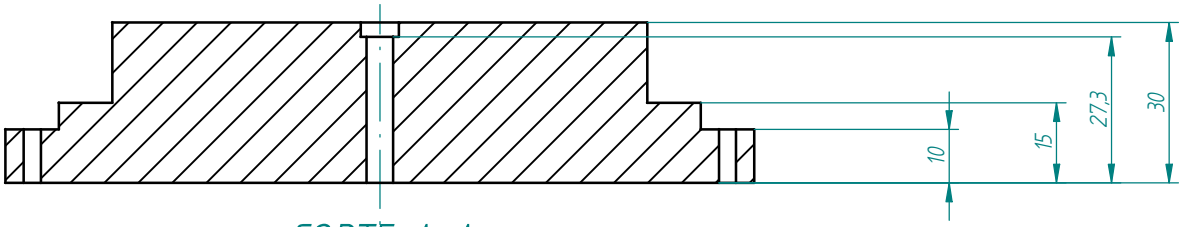

CORTE A-A

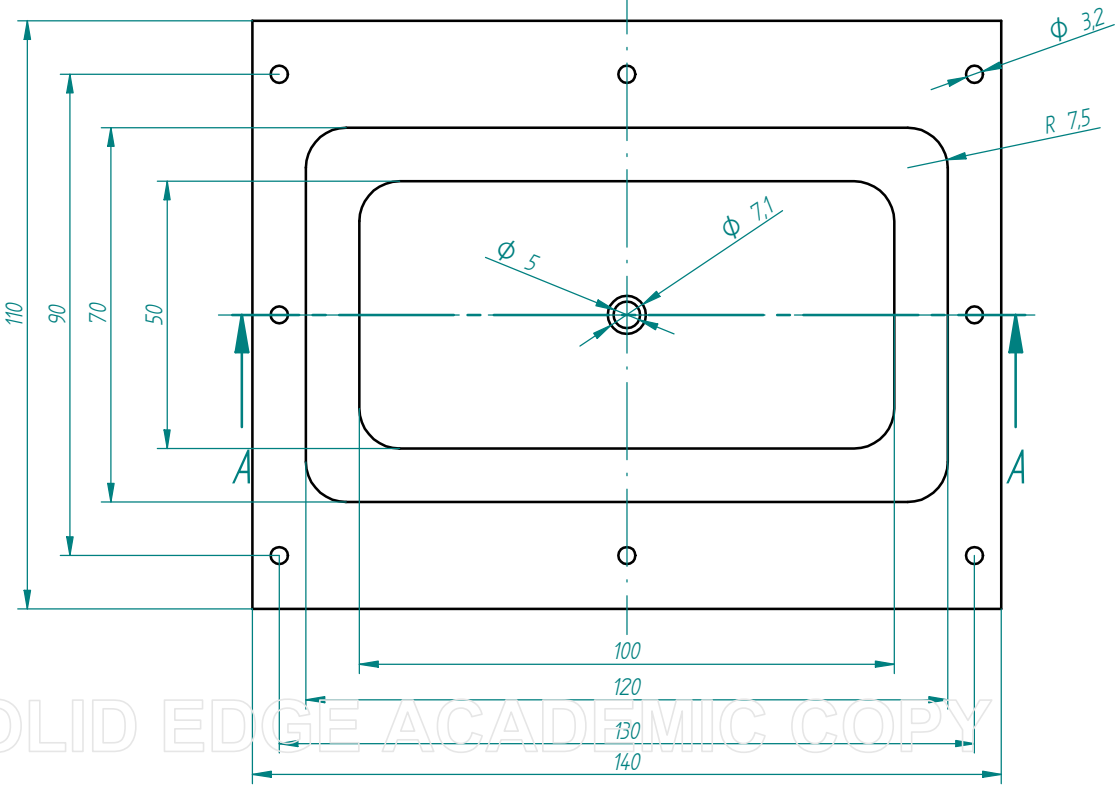

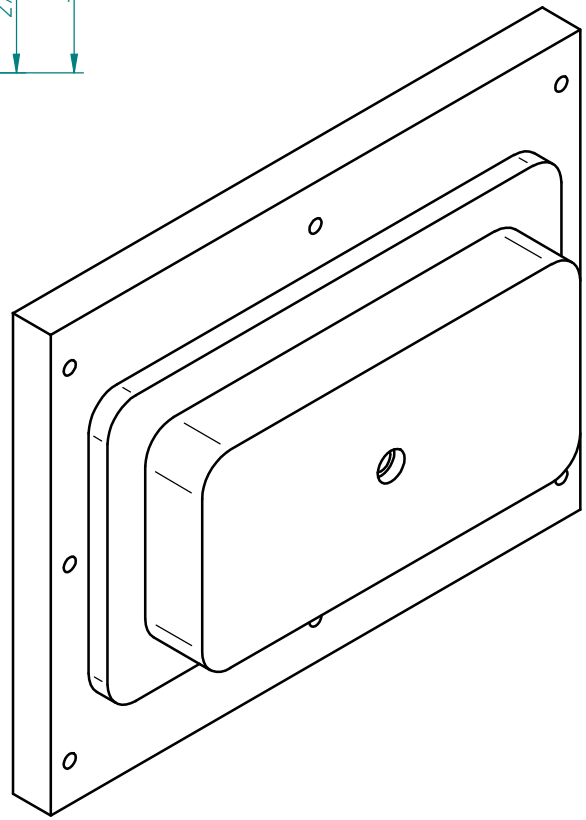

	Nombre	Fecha
Dibujado	Pablo Alejandro	16/04/18
Comprobado		
Aprobado 1		
Aprobado 2		

Salvo indicación contraria cotas en milímetros ángulos en grados tolerancias ±0,5 y ±1°

SOLID EDGE
EDS-PLM SOLUTIONS

Título

A3	Plano	Rev

Archivo: tapav4.dft

Escala	Peso	Hoja 1 de 1

Revisiones			
Rev	Descripción	Fecha	Aprobado

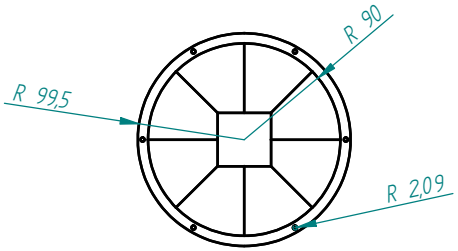

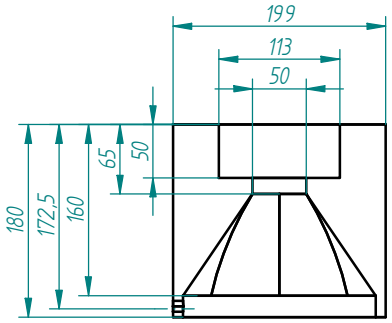

CORTE A-A

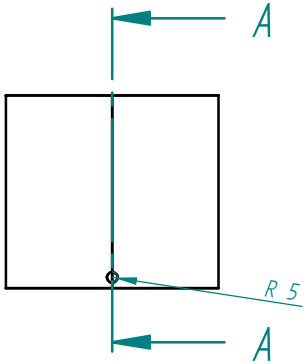

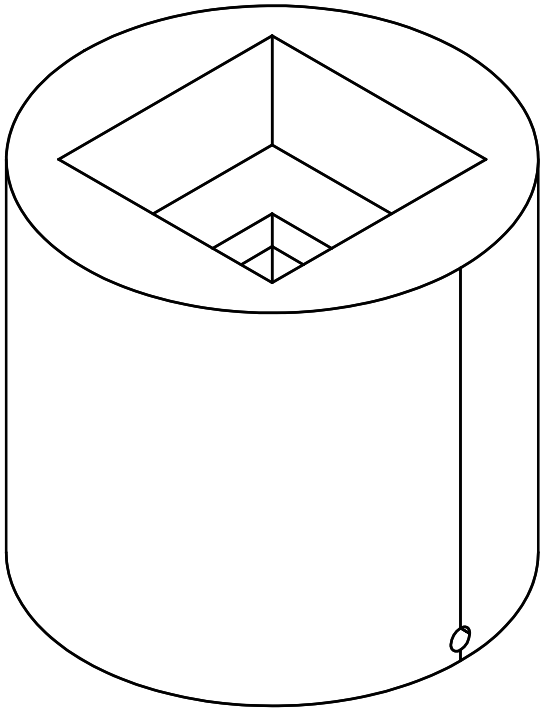

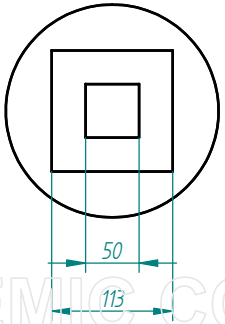

	Nombre	Fecha
Dibujado	Pablo Alejandro	13/08/18
Comprobado		
Aprobado 1		
Aprobado 2		

Salvo indicación contraria
cotas en milímetros
ángulos en grados
tolerancias ±0,5 y ±1°

SOLID EDGE
EDS-PLM SOLUTIONS

Título

A3	Plano	Rev

Archivo: ADAPTADORDEF INITIVO.dft

Escala	Peso	Hoja 1 de 1

Revisiones			
Rev	Descripción	Fecha	Aprobado

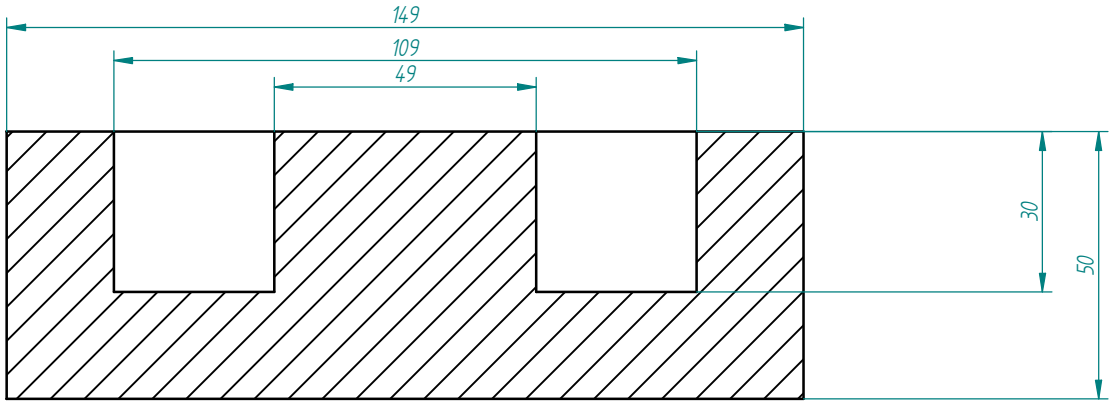

CORTE A-A

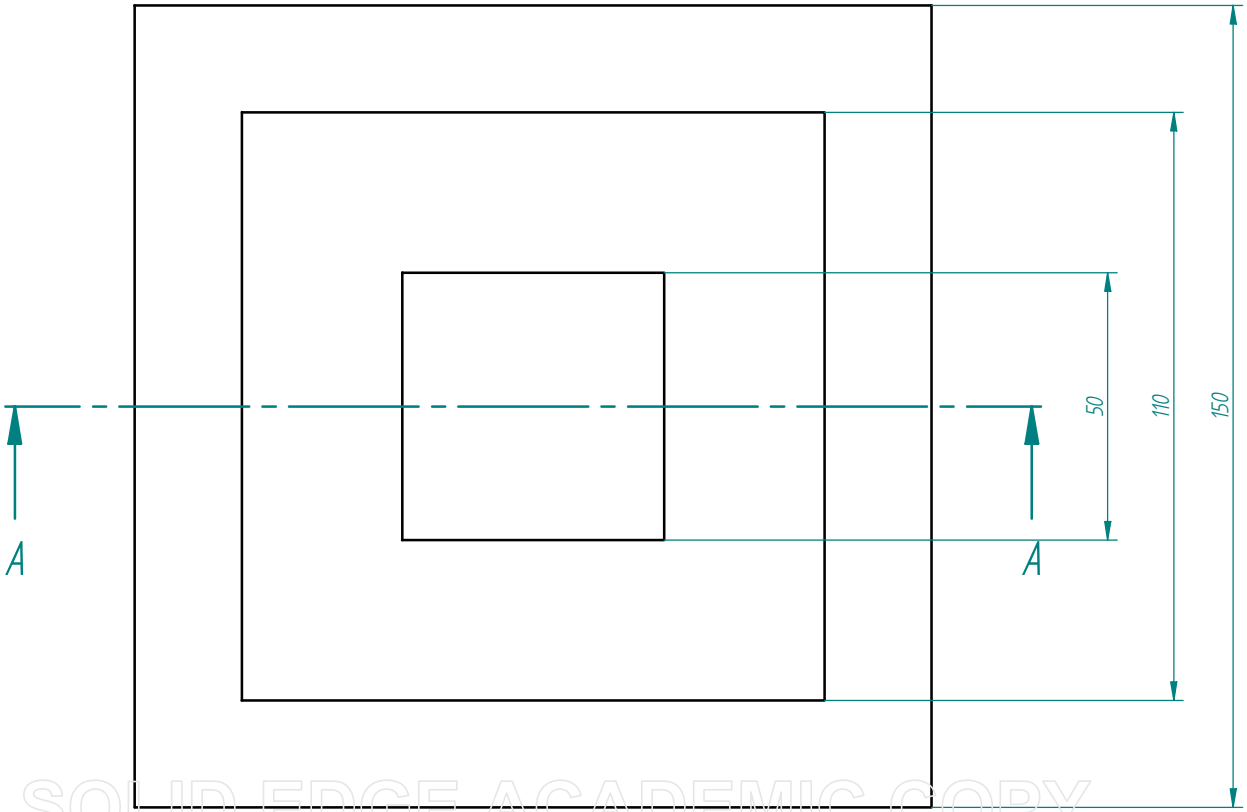

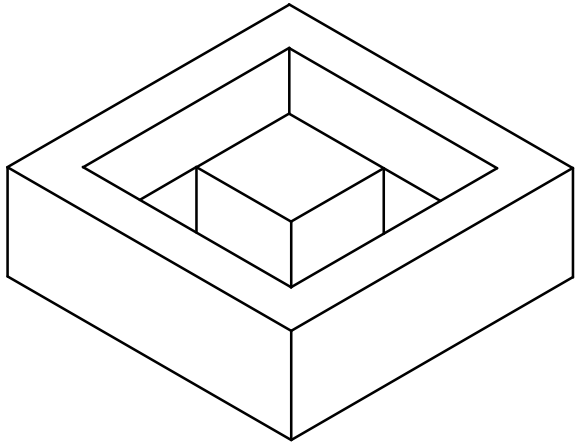

	Nombre	Fecha
Dibujado	Pablo Alejandro	30/06/18
Comprobado		
Aprobado 1		
Aprobado 2		

Salvo indicación contraria cotas en milímetros ángulos en grados tolerancias ±0,5 y ±1°

SOLID EDGE
EDS-PLM SOLUTIONS

Título

A3 | Plano | Rev

Archivo: Tapadeatras.dft

Escala | Peso | Hoja 1 de 1

Appendix C: Datasheets

PYLE®

SPEAKER SPECIFICATIONS

Model Number:	PLMRW8	
GENERAL SPECIFICATIONS		
Nominal Diameter:	8 inch	
Rated Lmpedance:	4 ohms	
Operating Bandwidth:	40-1.8k hz(-3dB)	
Power Handling Capacity:	200 Watts	
Sensitivity (1W/M):	88 dB(+-3dB)	
Voice Coil Diameter:	1.5 inch	
THIELE-SMALL PARAMRTERS		
Resonance Frequency	Fs:	36.6 HZ
DC Resistance	Re:	3.4ohm
Mechanical Q Factor	Qms:	3.2313
Electrical Q Factor	Qes:	0.502
Total Q Factor	Qts:	0.4345
Equivalent Cas air load	Vas:	33.97 L
Surface Area of Cone	Sd:	0.0216 m2
Efficiency Bandwidth Product	EBP	52.9
Voice Coil Over Hang	X-max	5.5 mm
PHYSICAL INFORMATION		
Basket:	Molded ABS Plastic Ba	
Magnet Type:	24 OZ	
Cone Material:	PP Cone	
Surround:	Rubber	

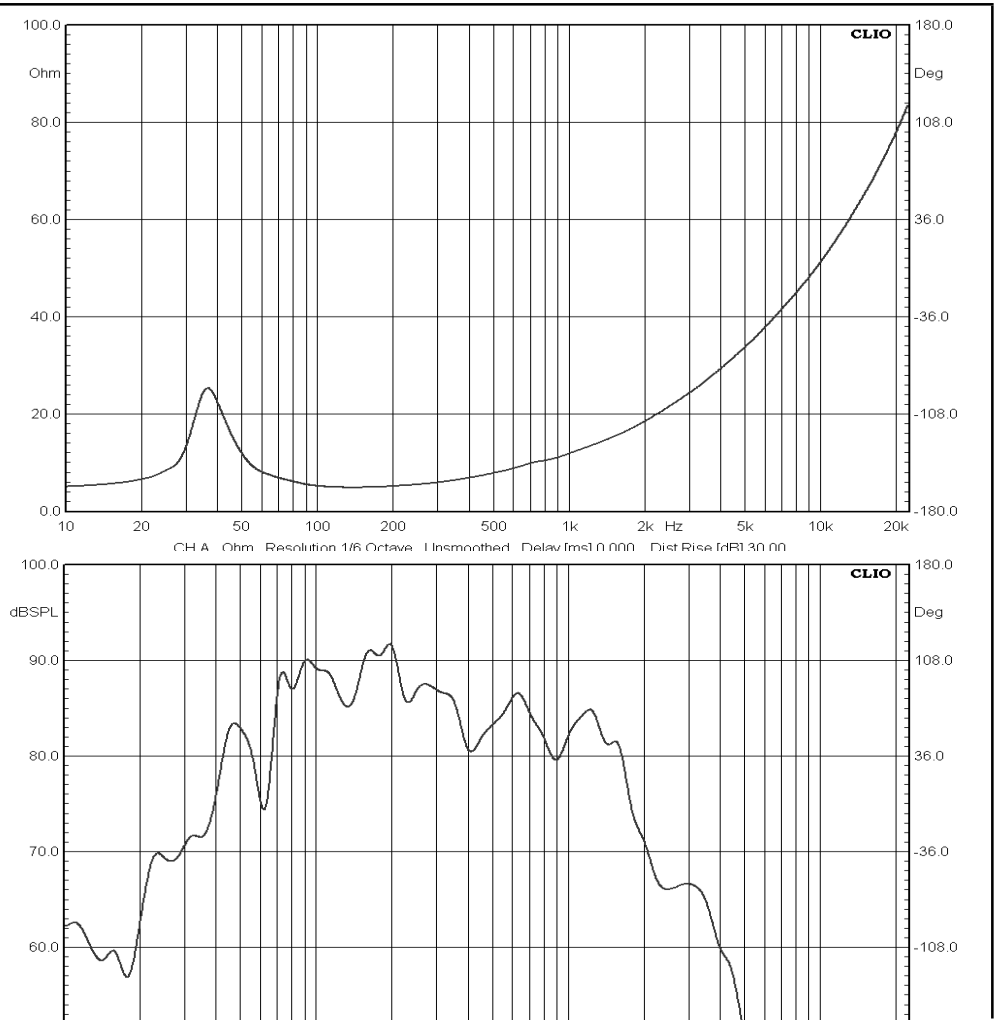

POW-1644L-LWC50-B-R
Omni-Directional Waterproof Microphone

3541 Stop Eight Road • Dayton, Ohio 45414

Product Overview

- 7.1mm overall diameter and 2.6mm height
- -44 dB sensitivity for use in most environments
- Wide 2 to 10 VDC operating voltage and 50-16,000 Hz frequency response
- >60 dB signal-to-noise ratio and 2.2 kOhm impedance
- Omni-directional polar pattern for great off-axis response
- IP57 rated and built with a rubber boot for a superior seal
- 50mm lead wires and a Molex® 51021-0200 connector

Typical Frequency Response and Sensitivity

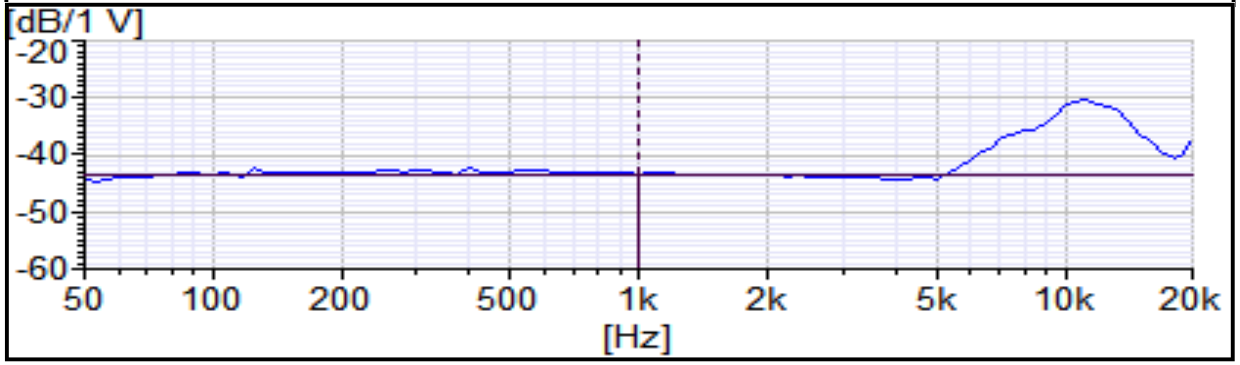

Appendix D: Test protocol

The following section is a general guide for future researchers in order to have an ordered and clear way to proceed with the experiments. Notice it is presented in a simple and generic way. As an illustrative example microphone calibration is used.

- **Test initiation:** perform an inventory. All the components should be present. For the case of the microphone calibration: loudspeaker, wiring, circuit components, signal generator, laptop and the microphone.
- **Set-up:** Assemble the test components carefully. For the example proposed Figures and could be taken as reference
- **Component check:** perform an initial test of the components both sources and sensors. For the case of the example. Play a simple tone in the loudspeaker and check that the microphone saves the result.
- **Safety check:** in every experiment there are some task that involve risk for the testers or people around it. Therefore safety procedures should be designed. For the case of the experiment, extremely dangerous sounds for the human ear are produced. Thus, a safety perimeter should be performed or protective headphones must be used.
- **Environment characterization:** if needed, record critical data of the experiment like ambient temperature or pressure.
- **Error sources:** record uncertainties of the measurements. It is needed to know at which extent results are accurate.
- **Test performance:** perform tests according to prior planning. Account for any unexpected event that may happen, for instance, in the experiment vibration of the supports of the loudspeaker due to resonance frequency crossing. This might help future researchers to understand the results.
- **Check convergence:** reproduce several times the same experiment in order to avoid unexpected or random failures.
- **Data collection:** save carefully the results indicating the parameters and conditions. For the case of the microphone, as an example: $Test\_2\_20Hz - 20kHz\_sweep\_300s$
- **Test end:** clean the zone and perform another inventory before saving all the components.